

RNA granule-clustered mitochondrial aminoacyl-tRNA synthetases form multiple complexes with the potential to fine-tune tRNA aminoacylation

Gui-Xin Peng^{1,2,†}, Xue-Ling Mao^{1,†}, Yating Cao³, Shi-Ying Yao¹, Qing-Run Li⁴, Xin Chen³, En-Duo Wang^{1,2,*} and Xiao-Long Zhou^{1,*}

¹State Key Laboratory of Molecular Biology, CAS Center for Excellence in Molecular Cell Science, Shanghai Institute of Biochemistry and Cell Biology, Chinese Academy of Sciences, University of Chinese Academy of Sciences, 320 Yue Yang Road, Shanghai 200031, China, ²School of Life Science and Technology, ShanghaiTech University, 393 Middle Hua Xia Road, Shanghai 201210, China, ³State Key Laboratory of Cellular Stress Biology, School of Life Sciences, Faculty of Medicine and Life Sciences, Xiamen University, Xiamen 361102, China and ⁴CAS Key Laboratory of Systems Biology, CAS Center for Excellence in Molecular Cell Science, Shanghai Institute of Biochemistry and Cell Biology, Chinese Academy of Sciences, 320 Yue Yang Road, Shanghai 200031, China

Received August 17, 2022; Revised October 23, 2022; Editorial Decision November 09, 2022; Accepted November 15, 2022

ABSTRACT

Mitochondrial RNA metabolism is suggested to occur in identified compartmentalized foci, i.e. mitochondrial RNA granules (MRGs). Mitochondrial aminoacyl-tRNA synthetases (mito aaRSs) catalyze tRNA charging and are key components in mitochondrial gene expression. Mutations of mito aaRSs are associated with various human disorders. However, the suborganelle distribution, interaction network and regulatory mechanism of mito aaRSs remain largely unknown. Here, we found that all mito aaRSs partly colocalize with MRG, and this colocalization is likely facilitated by tRNA-binding capacity. A fraction of human mitochondrial AlaRS (hmtAlaRS) and hmtSerRS formed a direct complex via interaction between catalytic domains *in vivo*. Aminoacylation activities of both hmtAlaRS and hmtSerRS were fine-tuned upon complex formation *in vitro*. We further established a full spectrum of interaction networks via immunoprecipitation and mass spectrometry for all mito aaRSs and discovered interactions between hmtSerRS and hmtAsnRS, between hmtSerRS and hmtTyrRS and between hmtThrRS and hmtArgRS. The activity of hmtTyrRS was also influenced by the presence of hmtSerRS. Notably, hmtSerRS utilized the same catalytic domain in mediating several interactions. Altogether, our results systematically analyzed the suborganelle localization and interac-

tion network of mito aaRSs and discovered several mito aaRS-containing complexes, deepening our understanding of the functional and regulatory mechanisms of mito aaRSs.

INTRODUCTION

Mitochondria play pivotal roles in various cellular activities; their main functions include performing oxidative phosphorylation (OXPHOS) to produce ATP, a process requiring five mitochondrial respiratory chain complexes (CI–CVs) located at the inner mitochondrial membrane (1,2). Human mitochondria have their own genome. Mitochondrial DNA (mtDNA), a closed circular double-stranded DNA with 16,569 base pairs, encodes 2 rRNAs (12S and 16S) and 22 tRNAs that decode 11 mRNAs for the translation of 13 mtDNA-encoded proteins, which compose the fundamental and essential subunits of complexes I, III, IV and V (3,4). Most mitochondrial proteins are encoded by nuclear DNA (nDNA), synthesized in the cytoplasm and posttranslationally imported into the mitochondria, including all other constituents of respiratory chain complexes (5), tRNA modification enzymes (6,7) and aminoacyl-tRNA synthetases (aaRSs) (8,9).

MtDNA associates with limited types of proteins to form a nucleoprotein complex called the mitochondrial nucleoid (10,11). Gene expression of mtDNA follows the ‘tRNA punctual model’ (3). mtDNA generates polycistronic precursors, which are processed into mono- or bi-cistronic mRNAs, most often via excision of flanking tRNAs by RNase P and RNase Z (12,13). Various steps in mtDNA

*To whom correspondence should be addressed. Tel: +86 21 5492 1247; Fax: +86 21 5492 1011; Email: xlzhou@sibcb.ac.cn
Correspondence may also be addressed to En-Duo Wang. Tel: +86 21 5492 1241; Fax: +86 21 5492 1011; Email: edwang@sibcb.ac.cn

†The authors wish it to be known that, in their opinion, the first two authors should be regarded as Joint First Authors.

gene expression, including replication, transcription, translation and degradation, coexist within the mitochondrial matrix; thus, it remains unclear how the functional compartmentalization of these steps is realized. Accumulating evidence supports that newly synthesized mitochondrial RNA is found in discrete foci and concentrated juxtaposed to nucleoids; these are termed mitochondrial RNA granules (MRGs) (14–16). The progress of nascent RNA transcription is tracked by immunofluorescence by labeling with the uridine analog 5-bromouridine (BrU) after a long pulse (17). Remarkably, G-rich sequence factor 1 (GRSF1), which is involved in RNA processing and translation, has a typical colocalization with the majority of BrU-labeled MRGs (14,15) and thus accordingly serves as an indicator for MRGs (15). To date, characterization of the MRG proteome has identified various proteins involved in post-transcriptional mitochondrial RNA metabolism, including tRNA metabolism-related proteins (RNase P, RNase Z) (14), pseudouridine synthases (TRUB2, RPUSD3, and RPUSD4), mRNA maturation and processing proteins (the members of FASTK family (18) and the mitochondrial poly(A)-polymerase (mtPAP) (19), rRNA methyltransferases (RNMTL1, MRM1, and MRM2) (20), ribosome assembly factors (16), and the hSuv3p-PNPase complex or degradosome (21,22). The presence of these RNA-related proteins in MRG suggests its central role in the posttranscriptional regulation of mitochondrial RNA metabolism, including RNA processing, ribosome biogenesis and assembly (23). However, as a recently identified suborganelle compartment, the intact proteome of MRG might still be incomplete.

AaRSs are divided into two classes (i.e. Classes I and II) based on the distinct structural motifs in the active site (24) and act as essential components in mRNA translation by generating aminoacyl-tRNAs. Human cells have 37 aaRS genes, encoding two sets of aaRSs for both cytoplasmic and mitochondrial mRNA translation (8,25) (in this manuscript, aaRSs are represented with three-letter amino acids with RS, e.g. SerRS represents seryl-tRNA synthetase). AaRSs from all species have conserved ancient catalytic domains. However, human cytoplasmic aaRSs (cyto aaRSs) frequently evolve N- or C-terminal extension in comparison to their bacterial homologs, which are usually not involved in substrate binding and catalysis but mediate protein–protein interactions (26,27). As such, nine aaRSs (cytoplasmic ArgRS, LeuRS, IleRS, MetRS, GluProRS, GlnRS, AspRS and LysRS) and three auxiliary factors (p43/AIMP1, p38/AIMP2 and p18/AIMP3) form a multiple-tRNA synthetase complex (MSC) (28,29). Notably, the presence of a terminal appendage is a prerequisite for most MSC constituents (30), except GlnRS and AspRS, which utilize catalytic domains for MSC targeting (31,32). In addition to human MSC, the formation of the aaRS-containing complex (sometimes a simplified MSC) is widespread in bacteria (such as bacteria AspRS/GlnRS-GatCAB amidotransferase; ProRS-YbaK in *Haemophilus influenzae* and *Escherichia coli*) (33), archaea (such as LeuRS-ProRS-LysRS in *Methanothermobacter thermautotrophicus*) (34) and lower eukaryotes (such as MetRS-Arc1p-GluRS in yeasts) (35); the presence of this complex is not

necessarily dependent on terminal appendages. In addition, human cyto aaRSs are frequently involved in various additional functions outside of translation, collectively called noncanonical functions (36). In parallel, there are nineteen nDNA-encoded mitochondrial aaRSs (mito aaRSs), except a tRNA synthetase producing Gln-tRNA^{Gln} (8). Compared with extensive studies of bacterial and cyto aaRSs, investigation of human mito aaRSs obviously lagged although a complete set of mito aaRSs was identified approximately two decades ago (25). However, we have witnessed a sharp explosion in the number of missense and nonsense mutations in mito aaRSs leading to various types of human disorders. These disorders occur at different stages in life and affect different tissues, particularly the high energy-consuming brain, muscle and heart (37,38). To date, nineteen mito aaRSs have been connected with human disorders, and more than 300 mutations in total mito aaRSs have been reported (37). However, the effect of the vast majority of these mutations on the structure and function of mito aaRSs remains unknown.

Most mito aaRSs are posttranslationally imported into mitochondria via an N-terminal mitochondrial targeting sequence (MTS) (37,39–41). The precise cleavage site of MTS of most mito aaRSs has not been experimentally established (40). However, inaccurate prediction of authentic mature mito aaRSs frequently leads to failure in gene expression in *Escherichia coli* due to the formation of protein aggregates. Therefore, only approximately half of mito aaRSs have been purified. To date, crystal structures of only human mitochondrial PheRS (hmtPheRS), hmtAspRS and hmtTyrRS have been examined (42–44). In addition, the suborganelle localization of mito aaRSs remains unclear despite previous studies identifying several mito aaRSs in the MRG proteome (45–47) and another reported inner membrane-associated hmtArgRS and hmtLysRS (*KARS1*-encoded mitochondrial isoform) (48). Furthermore, the interaction network of mito aaRSs remains unexplored, precluding the identification and investigation of their potential noncanonical functions, which has been reported for only hmtThrRS (49) and hmtTrpRS (50). In addition, considering widespread MSC in three domains of life, whether specific mito aaRSs form some types of MSC has never been reported.

In this study, we found that all mito aaRSs are partially localized in the MRG. Moreover, the tRNA binding capacity of mito aaRSs seems to confer their distribution in the MRG. We further found that a fraction of hmtAlaRS and hmtSerRS form a direct complex *in vivo*; the hmtAlaRS–hmtSerRS complex formation is able to fine-tune the tRNA charging activity of individual components. In addition, we performed immunoprecipitation and subsequent mass spectrometry (IP-MS) analyses for nineteen mito aaRSs and further identified several aaRS complexes and found that hmtSerRS is able to form multiple complexes using the same catalytic domain. In summary, our results systematically analyzed the cellular localization and interaction network of full sets of mito aaRSs and discovered several mito aaRS complexes, thereby deepening our understanding of the functional and regulatory mechanisms of mito aaRSs.

MATERIALS AND METHODS

Materials

T4 DNA ligase and Lipo8000 transfection reagent were purchased from Beyotime Biotechnology (Shanghai, China). $2 \times$ Taq Plus Master Mix (Dye Plus) and T4 polynucleotide kinase was purchased from Vazyme Biotechnology (Nanjing, China). The KOD-Plus Mutagenesis Kit and KOD-Plus Kit were from TOYOBO (Osaka, Japan). Ni²⁺-NTA Superflow resin was purchased from Qiagen Inc. (Hilden, Germany). Dynabeads Protein G, 4,6-diamidino-2-phenylindole (DAPI), MitoTracker, Pierce Silver Stain kit, and Alexa Fluor 488-conjugated secondary antibody were obtained from Thermo Scientific (Waltham, MA, USA). [¹⁴C]Thr, [¹⁴C]Ser and [¹⁴C]Tyr were obtained from Perkin Elmer Inc. (Waltham, MA, USA). PrimeScript RT Master Mix and PrimeSTAR Max DNA Polymerase were obtained from TaKaRa (Kyoto, Japan). Trelief Prestained Protein Ladder and oligonucleotide primers were obtained from Tsingke (Shanghai, China). Competent *E. coli* BL21(DE3) were purchased from Weidi Biotechnology (Shanghai, China). Serum-free Cell Cryopreservation Medium was obtained from Epizyme Biomedical Technology (Shanghai, China). Anti-c-Myc magnetic beads, kanamycin sulfate and ampicillin sodium were purchased from MedChemExpress (MCE, New Jersey, USA).

Antibodies

Anti-Myc (2276S) and anti-FLAG (14793S) were purchased from Cell Signaling Technology (Beverly, MA, USA). Anti-GRSF1 (HPA036985), HRP-labeled anti-mouse and anti-rabbit secondary antibodies were obtained from Sigma–Aldrich (St. Louis, MO, USA). Anti-His₆ (66005-1-Ig), anti-GAPDH (60004-1-Ig) and anti-hmtLeuRS (17097-1-AP) were purchased from Proteintech (Rosemont, IL, USA). Mature hmtAlaRS (Ser²⁶-Leu⁹⁸⁵) (9), hmtSerRS (Thr³⁵-Ser⁵¹⁸) (51) and hmtThrRS (Leu²⁰-Phe⁷¹⁸) (52) proteins were purified from *E. coli* and used as antigens to generate anti-hmtAlaRS, anti-hmtSerRS and anti-hmtThrRS antibodies, respectively (ABclonal, China).

Gene cloning, expression and protein purification

Constructs of genes expressing hmtAlaRS (encoded by *AARS2*), hmtLysRS (encoded by *KARS1*), hmtSerRS (encoded by *SARS2*) and hmtThrRS (encoded by *TARS2*) were constructed as described previously (9,51–53). Open reading frames (ORFs) of human hmtCysRS (encoded by *CARS2*), hmtGluRS (encoded by *EARS2*), hmtPheRS (encoded by *FARS2*), hmtIleRS (encoded by *IARS2*), hmtGlyRS (encoded by *GARS1*), hmtHisRS (encoded by *HARS2*), hmtLeuRS (encoded by *LARS2*), hmtMetRS (encoded by *MARS2*), hmtAsnRS (encoded by *NARS2*), hmtArgRS (encoded by *RARS2*), hmtProRS (encoded by *PARS2*), hmtValRS (encoded by *VARS2*), hmtTrpRS (encoded by *WARS2*) and hmtTyrRS (encoded by *YARS2*) were amplified from cDNA of HEK293T cells and inserted into various cleaved sites of pCMV-3Tag-3A

or pcDNA3.1 (with a C-terminal Myc tag) for gene expression in HEK293T cells. GRSF1 ORF was amplified from HEK293T cDNA and inserted between the BamHI and XhoI sites of pcDNA3.1 (with a C-terminal FLAG tag) for gene expression in HEK293T cells. The sequences encoding mature forms of hmtAlaRS (Ser²⁶-Leu⁹⁸⁵) (9) and hmtSerRS (Thr³⁵-Ser⁵¹⁸) (51) were separately cloned into multiple cloning sites 1 and 2 of the pRSFDuet-1 expression vector to generate pRSFDuet-hmtSerRS-His₆-hmtAlaRS for coexpression in *E. coli*; thus, mature hmtSerRS was expressed with an N-terminal His₆ tag (hmtSerRS-His₆), while hmtAlaRS was expressed without a tag. Similar procedures were used to generate pRSFDuet-hmtSerRS-His₆-hmtLeuRS (Ile⁴⁰-Asp⁹⁰³), pRSFDuet-hmtAsnRS (Ser²⁵-Leu⁴⁷⁷)-His₆-hmtSerRS, pRSFDuet-hmtTyrRS (Ala³²-Leu⁴⁷⁷)-His₆-hmtSerRS and pRSFDuet-hmtArgRS (Met¹-Met⁵⁷⁸)-His₆-hmtThrRS (Leu²⁰-Phe⁷¹⁸). A fragment encoding mature hmtAlaRS was inserted into pET30a with an N-terminal His₆ tag as described in a previous report (9). Gene mutagenesis was performed according to the protocol provided with the KOD Plus Mutagenesis Kit. Constructs of hmtAlaRS-ΔC (Met¹-Gly⁷⁸³, with deletion of Glu⁷⁸⁴-Leu⁹⁸⁵), hmtLeuRS-ΔC (Met¹-Gln⁸³⁴, with deletion of Gln⁸³⁵-Asp⁹⁰³), hmtSerRS-ΔN (Met¹-Ser⁵¹⁸, with deletion of Thr³⁵-Pro¹⁷¹) and hmtThrRS-ΔC (Met¹-Phe⁶¹⁴, with deletion of Pro⁶¹⁵-Phe⁷¹⁸) were generated using a KOD Plus Mutagenesis Kit. All primer sequences are listed in Supplementary Table S1.

For expression, the relevant construct was transformed into *E. coli* BL21 (DE3) cells, which were induced with a final concentration of 100 μM IPTG at 18°C for 10 h. Proteins were purified by Ni²⁺-NTA Superflow resin according to the manufacturer's protocol. hmtAlaRS-His₆ was further purified by gel filtration on a Superdex 200 column with 50 mM Tris-HCl (pH 8.0) and 150 mM NaCl, while hmtSerRS-His₆ was applied on a Superdex 75 column with 50 mM Tris-HCl (pH 8.0), 150 mM NaCl and 5 mM β-ME. Purification of mature hmtTyrRS (Ala³²-Leu⁴⁷⁷) and hmtLeuRS (Ile⁴⁰-Asp⁹⁰³) were performed as described previously (25,54). All purified proteins were concentrated and stored at -20°C after mixing with an equal volume of glycerol. The protein concentrations were determined by using a BCA kit.

Cell transfection, coimmunoprecipitation (Co-IP) and western blot

Human embryonic kidney 293T (HEK293T) cells were transfected by using Lipo8000 transfection reagent according to the manufacturer's protocol. After transfection for 24 h, the cells were washed with ice-cold phosphate-buffered saline (PBS) three times and lysed in 500 μl of RIPA buffer (50 mM Tris-HCl (pH 7.5), 150 mM NaCl, 0.5% sodium deoxycholate, 1% Triton X-100, 0.1% SDS) supplemented with a protease inhibitor cocktail for 25 min at 4°C. Co-IP and western blot were performed as described previously (6).

Mito aaRS copurification in *E. coli*

Plasmids and methods for *E. coli* coexpression were performed as described above. The *E. coli* cells were lysed by

sonication in lysis buffer containing 50 mM Tris-HCl (pH 8.0), 300 mM NaCl, 10% glycerol, and 10 mM imidazole and then centrifuged at 16 000 g at 4°C for 1 h. The supernatant was incubated with Ni²⁺-NTA Superflow resin at 4°C for 45 min, washed with 30 ml lysis buffer plus 20 mM imidazole, and finally eluted in lysis buffer plus 250 mM imidazole. The eluate was collected for western blot analysis.

Silver staining

IP was performed using HEK293T whole cell lysate (WCL) overexpressing a given mito aaRS. The pCMV-3Tag-3A empty plasmid was expressed as a control. The precipitated sample was separated by SDS-PAGE and visualized with silver staining to check the sample quality. Qualified eluted samples were analyzed by liquid chromatography-mass spectrometry (LC-MS). The results were analyzed, and the first 10 enriched proteins were presented in this study according to the protein intensity in corresponding aaRS versus control precipitates.

tRNA gene cloning and transcription

A plasmid harboring the human mitochondrial tRNA^{Ala} (hmtRNA^{Ala}) gene was constructed as described previously (9). Genes encoding hmtRNA^{Ser}(AGY), hmtRNA^{Ser}(UCN) and hmtRNA^{Tyr} were incorporated into a pTrc99b plasmid. All hmtRNAs were produced by *in vitro* transcription using a T7 RNA polymerase S43Y mutant (55) as described previously (9). The primers for tRNA transcription are listed in Supplementary Table S1.

Aminoacylation assays

Aminoacylation of hmtRNA^{Ala} were performed in a reaction mixture containing 50 mM Tris-HCl (pH 8.0), 20 mM KCl, 10 mM MgCl₂, 2 mM DTT, 4 mM ATP, 50 μM [¹⁴C]Ala, 5 μM hmtRNA^{Ala} and 200 nM mature hmtAlaRS or in the presence of various concentrations of mature hmtSerRS-R330A (hmtAlaRS to hmtSerRS-R330A ranging from 1:1 to 1:8) at 37°C. Aminoacylation of hmtRNA^{Ser}(AGY) or hmtRNA^{Ser}(UCN) was measured in a reaction mixture containing 50 mM Tris-HCl (pH 7.5), 60 mM KCl, 15 mM MgCl₂, 5 mM DTT, 2.5 mM ATP, 181 μM [¹⁴C]Ser, 10 μM hmtRNA^{Ser}(AGY) or hmtRNA^{Ser}(UCN), 500 nM mature hmtSerRS or at the presence of various concentrations of mature hmtAlaRS-R110A (hmtSerRS/hmtAlaRS-R110A ranging from 1:1 to 1:8) or at the presence of various concentrations of mature hmtTyrRS (hmtSerRS/hmtTyrRS ranging from 1:1 to 1:8) or at the presence of various concentrations of mature hmtLeuRS (hmtSerRS/hmtLeuRS ranging from 1:1 to 1:8) at 37°C. Aminoacylation of hmtRNA^{Tyr} was measured in a reaction mixture containing 50 mM Tris-HCl (pH 8.0), 25 mM KCl, 12 mM MgCl₂, 5 mM DTT, 2.5 mM ATP, 0.2 mg/ml BSA, 200 μM [¹⁴C]Tyr, 10 μM hmtRNA^{Tyr} and 500 nM mature hmtTyrRS or in the presence of various concentrations of mature hmtSerRS (hmtTyrRS/hmtSerRS ranging from 1:1 to 1:8). The two enzymes described above were incubated at 4°C for 30 min prior to the aminoacylation assay. All the samples were processed as described previously (56).

Immunofluorescence (IF)

The specific plasmids were overexpressed in HEK293T cells. After 24 h, the cells were fixed in 4% paraformaldehyde (PFA) for 25 min at room temperature. Fixed cells were blocked and permeabilized in PBS plus 0.1% Triton X-100 buffer containing 5% BSA for 2 h and incubated with the indicated primary antibodies overnight at 4°C. The cells were immunostained with Alexa Fluor 488-conjugated and cyanine 3 (Cy3)-conjugated secondary antibodies for 1 h, and the nuclei were counterstained with DAPI for 5 min at room temperature. Fluorescence images were captured with a Leica TCS SP8 confocal microscope or Zeiss LSM 980 Airyscan superresolution microscope.

Gel filtration chromatography of cell lysates

HEK293T WCL, mature hmtAlaRS-His₆ and hmtSerRS-His₆ were applied to a Superose 6 column for high-performance liquid chromatography (HPLC) and eluted at a flow rate of 0.5 ml/min by using a buffer containing 50 mM Tris-HCl (pH 8.0), 50 mM NaCl, and 1 mM phenyl methylsulfonyl fluoride (PMSF). Fractions were collected for analysis by western blot.

Reconstruction of the hmtAlaRS-hmtSerRS complex

Equal amounts (300 μg) of purified mature hmtAlaRS-His₆ and hmtSerRS-His₆ were incubated in a buffer containing 50 mM Tris-HCl (pH 8.0), 60 mM KCl, 10 mM MgCl₂, 5 mM DTT, and 4 mM ATP at 4°C for 30 min and then applied to a Superdex 200 10/300 GL column in running buffer containing 50 mM Tris-HCl (pH 8.0), 50 mM NaCl and 5 mM β-ME. Fractions were collected for analysis by SDS-PAGE.

RESULTS

Analyses of primary sequences of human mito aaRSs

As stated above, cyto aaRSs usually contain terminal appendages to mediate protein-protein interactions in MSC formation and other noncanonical functions. We analyzed primary sequences and any potential terminal extensions in mito aaRSs. Note that MTSs of some mito aaRSs have been experimentally established, while those of others remain unclear (37,40,41,57,58). Based on detailed primary sequence alignment, domains in crystal structures of hmtPheRS (42), hmtAspRS (43), hmtTyrRS (44), GlyRS (cytoplasmic isoform) (59), LysRS (cytoplasmic isoform) (60), comparison with crystal structures of bacterial aaRSs, or predicted structures obtained by AlphaFold 2 (61,62), we defined various domains of all mito aaRSs (Figure 1). The results showed that, in the primary sequence, most mito aaRSs more resemble their bacterial counterparts than cyto aaRSs, in line with the bacterial origin of mitochondria, and thus harbor no terminal appendages. For some specific aaRSs, compared with bacterial ThrRS, hmtThrRS more resembles cytoplasmic ThrRS in sequence and contains an N-terminal extension approximately 40 amino acids in length, whose function remains unclear. Mitochondrial and

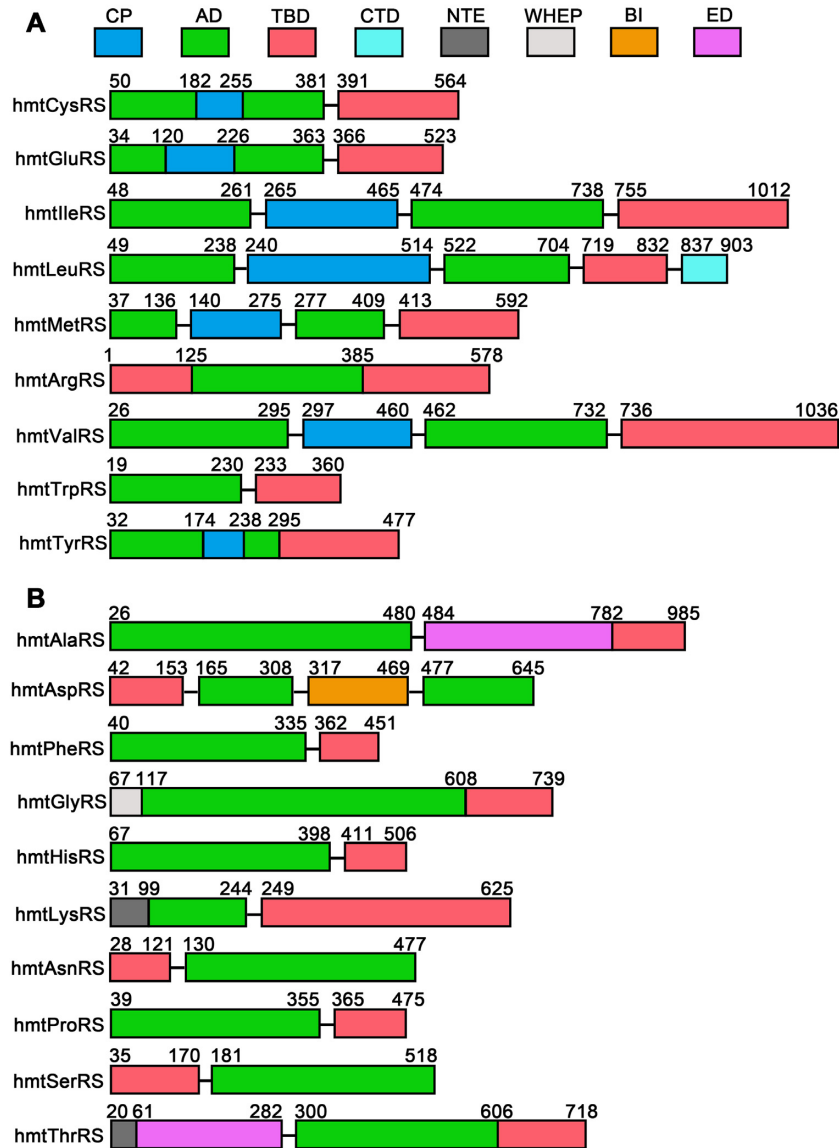


Figure 1. Schematic representation of all mito aaRS domain compositions. (A, B) Mito aaRSs were classified into two types, including nine Class I (A) and ten Class II aaRSs (B). CP, connective polypeptide; AD, aminoacylation domain; TBD, tRNA binding domain; CTD, C-terminal domain; NTE, N-terminal extension; BI, bacterial insertion; ED, editing domain.

cytoplasmic GlyRSs are encoded by the same gene, *GARS1*, via translational reinitiation (63); thus, the mitochondrial version of GlyRS has an N-terminal WHEP domain, which is also present in cytoplasmic TrpRS, HisRS and GluProRS (26). In parallel, mitochondrial and cytoplasmic LysRSs are encoded by the same gene, *KARS1*, via mRNA alternative splicing (64); thus, the mitochondrial version of LysRS harbors an N-terminal extension, which has been shown to be a tRNA^{Lys} binding element (65). In addition, hmtAspRS contains a bacterial type insertion domain, which is absent in cytoplasmic AspRS, which has been modeled to potentially bind the tRNA acceptor stem (43). Notably, hmtProRS lacks an INS editing domain found in bacterial ProRS. hmtPheRS is a chimera of α - and β -subunits of its cytoplasmic counterpart and is likely an editing-deficient

aaRS similar to its yeast counterpart (66). Furthermore, the CP1 editing domain of hmtLeuRS was degenerate with a mutated active site and obviously truncated compared with bacterial LeuRS or cytoplasmic LeuRS. Indeed, we and others have shown that hmtLeuRS is unable to hydrolyze mischarged tRNA^{Leu}, but the truncated CP1 domain is important for tRNA^{Leu} aminoacylation (67,68). In contrast, two other aaRSs from Class Ia, hmtIleRS and hmtValRS, have an intact editing domain and conserved active site, suggesting that they are editing-capable aaRSs.

In summary, most mito aaRSs resemble their bacterial homologs with no obvious terminal extensions, except hmtThrRS, hmtGlyRS, hmtLysRS and hmtAspRS, which harbor N-terminal extensions or insertion domains (Figure 1).

All mito aaRSs partly localize in the MRG

Some mito aaRSs, including hmtAlaRS, hmtAspRS, hmt-TrpRS, hmtHisRS, hmtTyrRS, hmtSerRS, hmtThrRS, hmtIleRS and hmtArgRS, have been identified in the MRG proteome based on mass spectrometry analysis of enriched products of overexpressed GRSF1 or FASTKD2 (45–47). These results indicated that mito aaRSs potentially localized in the MRG but without further experimental evidence. GRSF1 is an indicator of MRG (14,15). Therefore, we selected GRSF1 as an MRG IF marker to investigate the potential colocalization of MRGs and mito aaRSs. Each mito aaRS gene was expressed with a C-terminal FLAG tag in HEK293T cells, which were then immunostained with anti-FLAG and anti-GRSF1 antibodies and observed by confocal microscopy, which is a widely used method to study MRG-localized proteins (18,45–47). We first chose hmtIleRS, hmtLeuRS, hmtArgRS, hmtTyrRS and hmtAlaRS, hmtAsnRS, hmtSerRS, hmtThrRS, which belong to Class I and Class II aaRSs, respectively. IF results showed that the above aaRSs exhibit discrete foci and have a clear colocalization with GRSF1 (Figure 2A, 2B). We further tested the colocalization of the remaining Class I and Class II aaRSs with MRGs in HEK293T cells and found that they also formed distinct foci and mostly colocalized with GRSF1 (Supplementary Figures S1A, 1B). Western blot analysis showed that all mito aaRS genes expressed proteins with correct sizes in HEK293T cells (Supplementary Figure S1C).

We further surveyed the potential colocalization of native mito aaRSs with MRG. Due to the fact that available antibodies for mito aaRSs and GRSF1 were all produced in rabbits, we overexpressed a C-terminal FLAG-tagged GRSF1 (GRSF1-FLAG) in HEK293T cells. The cells were then immunostained with anti-FLAG (produced from mice) and anti-hmtSerRS or anti-hmtThrRS antibodies. We found that native hmtSerRS and hmtThrRS indeed formed distinct foci and colocalized with overexpressed GRSF1 very well (Supplementary Figure S2).

Considering the limitation of resolution of confocal microscopy (~200 nm), we further applied superresolution microscopy (with a resolution of ~80 nm) to examine the spatial localization of mito aaRSs and MRGs. We selected several mito aaRSs, including hmtIleRS, hmtLeuRS, hmtAlaRS, hmtSerRS and hmtThrRS, as representatives. Fluorescence results showed that, with better resolution, these mito aaRSs are more dispersed but clearly colocalize with GRSF1-positive foci (Figure 3), which is in agreement with the above results from confocal microscopy (Figure 2A, 2B). In summary, the above results showed that mito aaRSs are indeed enriched in the MRG.

tRNA binding capacity likely confers mito aaRSs in the MRG

Although several RNA-related proteins have been identified in the MRG, the reason for MRG targeting is less understood. Considering that mitochondrial tRNAs are transcribed, posttranscriptionally processed in the MRG and charged by mito aaRSs, we reasoned that efficient tRNA binding might account for MRG enrichment of mito

aaRSs. To explore this possibility, it is necessary to obtain several mutants with impaired tRNA binding capacity. Based on our above sequence and domain analysis, the C-terminal domains of hmtAlaRS, hmtLeuRS, and hmtThrRS and the N-terminal domain of hmtSerRS are well-established key tRNA binding elements based on the structures of their homologs (Supplementary Figure S3). Therefore, we constructed genes encoding hmtAlaRS- Δ C, hmtLeuRS- Δ C, hmtSerRS- Δ N and hmtThrRS- Δ C mutants whose tRNA binding domains were deleted. TIM23, a protein located in the mitochondrial inner membrane, was introduced as a negative control. Indeed, TIM23 showed little colocalization with GRSF1 (Supplementary Figure S4A). hmtAlaRS- Δ C, hmtLeuRS- Δ C and hmtSerRS- Δ N were found to be diffused in the mitochondrial matrix, and hmtThrRS- Δ C was hardly enriched with GRSF1 foci despite being organized into distinct foci (Supplementary Figure S4A). The aaRS mutants were expressed in HEK293T cells with the correct molecular masses (Supplementary Figure S4B). Therefore, these observations suggested that tRNA binding capacity confers mito aaRSs in the MRG and that the tRNA-binding domain is a determinant for mito aaRS import into the MRG.

A fraction of hmtAlaRS and hmtSerRS interact directly *in vivo*

AaRS-containing complexes have been found in bacteria, archaea, and eukaryotic cytoplasm. All mito aaRSs are clustered in the MRG foci. These results prompted us to explore whether some types of MSCs exist in human mitochondria. We initially selected hmtAlaRS because we recently purified the mature form of hmtAlaRS, reconstituted its aminoacylation and editing activities, elucidated its tRNA recognition pattern, revealed the essential role of its editing of mischarged tRNA^{Ala} in mammalian embryonic development and clarified the mechanism of hmtAlaRS R580W-associated heart diseases (9,69,70). We overexpressed a gene encoding a C-terminal FLAG-tagged hmtAlaRS (hmtAlaRS-FLAG) and performed an IP assay (Supplementary Figure S5A). Then, the precipitated product was analyzed using LC–MS to identify unknown interacting proteins. Among these potential interacting proteins, *SARS2*-encoded hmtSerRS and *TARS2*-encoded hmtThrRS were among the top list (Supplementary Figure S5B). We then performed a similar IP in combination with LC–MS (IP–MS) by overexpressing C-terminal FLAG-tagged hmtSerRS (hmtSerRS-FLAG) or hmtThrRS (hmtThrRS-FLAG). Indeed, hmtAlaRS was enriched in the precipitated samples of hmtSerRS-FLAG (Supplementary Figure S5C); however, hmtArgRS but not hmtAlaRS was detected in the precipitated product of hmtThrRS-FLAG (Supplementary Figure S5D). Therefore, using this method, hmtAlaRS and hmtSerRS could be mutually pulled down.

Based on the above IP–MS results, we coexpressed genes encoding hmtAlaRS-FLAG and hmtSerRS with a C-terminal Myc tag (hmtSerRS-Myc) in HEK293T cells and performed Co-IP with an anti-FLAG antibody. The results showed that hmtSerRS-Myc coprecipitated with hmtAlaRS-FLAG (Figure 4A). Additionally, using an anti-

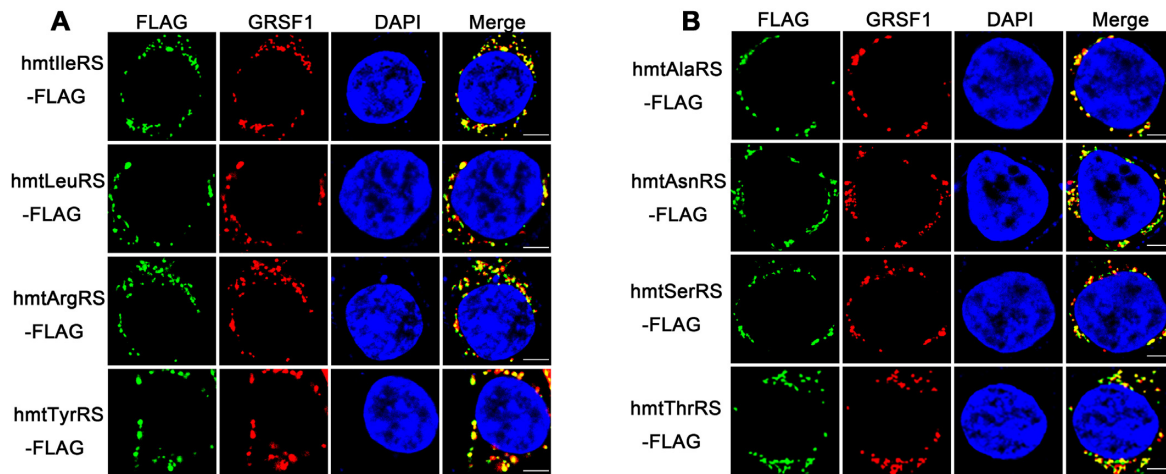


Figure 2. Mito aaRSs colocalize with GRSF1. (A, B) Confocal analysis of the colocalization of overexpressed Class I (A) or Class II (B) mito aaRSs and endogenous GRSF1 in HEK293T cells. The cells were transfected with plasmids encoding the FLAG-tagged proteins indicated and then immunolabeled with anti-FLAG and anti-GRSF1 antibodies. The nucleus was stained with DAPI. Scale bars: 10 μ m.

Myc antibody in the Co-IP assay, hmtAlaRS-FLAG was pulled down by hmtSerRS-Myc (Figure 4B). These results clearly showed that hmtAlaRS and hmtSerRS could form a complex. To further confirm the interaction between endogenous hmtAlaRS and hmtSerRS *in vivo*, we prepared hmtAlaRS antibody (anti-hmtAlaRS) and hmtSerRS antibody (anti-hmtSerRS) (see Materials and Methods). We performed Co-IP assays using anti-hmtSerRS or anti-hmtAlaRS antibody and HEK293T WCL. The results revealed that endogenous hmtAlaRS was precipitated by hmtSerRS (Figure 4C). Similarly, endogenous hmtSerRS was enriched by hmtAlaRS (Figure 4D).

To exclude nonspecific interaction, we included hmtLeuRS as a negative control, which was not identified in hmtSerRS IP-MS assay. Genes encoding hmtLeuRS with a C-terminal FLAG tag (hmtLeuRS-FLAG) and hmtSerRS-Myc were expressed in HEK293T cells. Using an anti-Myc antibody to perform Co-IP, hmtLeuRS-FLAG was not coprecipitated with hmtSerRS-Myc (Supplementary Figure S6A), suggesting that hmtSerRS-hmtAlaRS interaction was specific.

To investigate whether the interaction between hmtAlaRS and hmtSerRS is direct, the genes encoding mature hmtSerRS with an N-terminal His₆ tag (hmtSerRS-His₆) and mature hmtAlaRS without a tag were introduced into the *E. coli* dual expression vector pRSFDuet-1. After gene expression in *E. coli*, we found that mature hmtAlaRS could be copurified with mature hmtSerRS-His₆ using Ni-NTA affinity chromatography (Supplementary Figure S7A). Similar analysis was performed to confirm that hmtSerRS-His₆ had no interaction with untagged hmtLeuRS in *E. coli* (Supplementary Figure S6B). Furthermore, to more prove the direct interaction of hmtAlaRS and hmtSerRS, equal molar amounts of purified His₆-tagged hmtAlaRS (hmtAlaRS-His₆) and hmtSerRS-His₆ were mixed, and then, Co-IP was performed using anti-hmtSerRS antibody. Western blot analysis showed that hmtAlaRS-His₆ was indeed coprecipitated with hmtSerRS-His₆ (Supplementary Figure S7B). These evidences explicitly demonstrated that

hmtAlaRS and hmtSerRS directly interact *in vitro* and *in vivo*.

We have reported that hmtAlaRS is monomeric *in vivo* (9). Others have reported that bovine mitochondrial SerRS is a dimer (71). Based on the fact that hmtAlaRS and hmtSerRS formed a complex *in vivo*, it is expected that endogenous hmtAlaRS and hmtSerRS would be eluted at a larger molecular mass in gel filtration. Thus, gel filtration chromatography was subsequently performed to analyze HEK293T WCL to check whether endogenous hmtAlaRS and hmtSerRS were distributed in larger entities. We first analyzed the elution fraction of purified mature hmtAlaRS-His₆ and hmtSerRS-His₆ on a Superose 6 column using an anti-His₆ antibody. The data showed that both proteins eluted at similar volumes (Figure 4E), consistent with their comparable molecular masses (hmtAlaRS-His₆ monomer, ~108 kDa *vs.* hmtSerRS-His₆ dimer, ~116 kDa). Then, HEK293T WCL was loaded on a Superose 6 column (Figure 4E), samples at different elution times were collected, and western blot analysis was performed with either anti-hmtAlaRS or anti-hmtSerRS antibody. The results showed that the vast majority of hmtAlaRS exists as a monomer *in vivo* (Figure 4E); however, a small fraction of hmtAlaRS was indeed present in larger molecular masses. Likewise, despite the existence of dimeric hmtSerRS, a significant amount of hmtSerRS was present as larger and variable molecular entities (Figure 4E). Therefore, these data indicated that at least a portion of endogenous hmtAlaRS and hmtSerRS are prone to form complexes *in vivo*.

Based on the crystal structure of bovine mitochondrial SerRS (PDB: 1WLE), hmtSerRS consists of an N-terminal α -helical tRNA binding domain (TBD) and a C-terminal aminoacylation domain (AD) (Figure 4F, top panel). Genes encoding the C-terminal Myc-tagged TBD of hmtSerRS (hmtSerRS-TBD-Myc) or the AD of hmtSerRS (hmtSerRS-AD-Myc) and hmtAlaRS-FLAG were coexpressed in HEK293T cells. Co-IP analysis showed that the AD domain of hmtSerRS is responsible for the hmtSerRS and hmtAlaRS interaction (Figure 4F, bottom panel). The

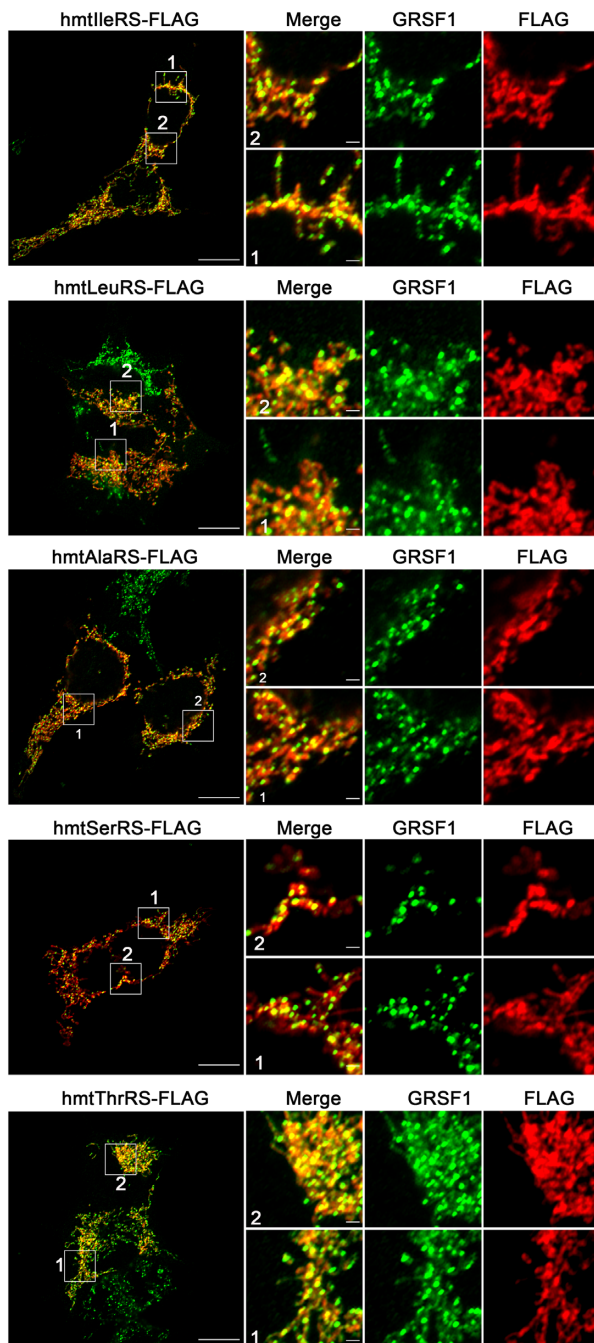


Figure 3. Mito aaRSs partially localize in the MRG. Fluorescence images of FLAG-tagged hmtIleRS, hmtLeuRS, hmtAlaRS, hmtSerRS, hmtThrRS and endogenous GRSF1 in HEK293T cells, which were obtained by superresolution. Scale bars: main, 10 μm ; inset, 1 μm .

structure of hmtAlaRS has not been determined; based on the archaea AlaRS structure (PDB: 3WQY) and predicted hmtAlaRS structure by AlphaFold 2, hmtAlaRS is composed of an N-terminal AD domain, a middle editing domain (ED) and a C-terminal tRNA binding domain (CD) (Figure 4G, top panel). Genes encoding C-terminal FLAG-tagged hmtAlaRS- ΔAD , hmtAlaRS- ΔED , or hmtAlaRS- ΔCD were coexpressed with hmtSerRS-Myc in HEK293T

cells. Co-IP results showed that deletion of the AD domain of hmtAlaRS abolished this interaction, revealing that hmtAlaRS-AD is responsible for the hmtAlaRS and hmtSerRS interaction (Figure 4G, bottom panel).

In summary, all the above data clearly showed that hmtAlaRS and hmtSerRS directly interact with each other *in vivo*, mediated by the aminoacylation domain in individual components.

Complex formation fine-tunes the tRNA aminoacylation activities of both hmtAlaRS and hmtSerRS

Subsequently, we tried to reconstitute the hmtAlaRS-hmtSerRS complex to understand the stoichiometry and function. The purified hmtAlaRS-His₆ and hmtSerRS-His₆ were incubated at equal amounts and then analyzed by gel filtration chromatography to explore whether they are able to form a stable complex *in vitro*. After incubation, the majority of each protein still eluted as free forms (Figure 5A); however, a small but observable peak between 9–11 ml (Figure 5A), with a larger absorbance value when compared with the free form of the individual component, containing both hmtAlaRS-His₆ and hmtSerRS-His₆, emerged (Figure 5B). Specifically, free hmtSerRS-His₆ was absent in the corresponding position (9–11 ml) (Figure 5C), suggesting that the presence of hmtSerRS-His₆ between 9–11 ml resulted from complex formation with hmtAlaRS-His₆. However, the small peak after incubation *in vitro* indicated that the affinity between hmtAlaRS-His₆ and hmtSerRS-His₆ under this condition was weak, consistent with the observation that the majority of endogenous hmtAlaRS and hmtSerRS eluted as free forms *in vivo* (Figure 4E).

We further explored the effect of complex formation on the aminoacylation of hmtAlaRS and hmtSerRS. Due to the weak interaction between the two proteins, we were unable to obtain a stable and homogeneous complex. We initially determined the effect of hmtAlaRS on tRNA charging by hmtSerRS. hmtSerRS has two tRNA substrates, hmtRNA^{Ser}(AGY) and hmtRNA^{Ser}(UCN). We have previously revealed that hmtAlaRS is able to significantly misactivate noncognate Ser (9). To prevent the indirect influence of Ser-AMP produced by hmtAlaRS on hmtSerRS activity, we mutated the absolutely conserved Arg110 residue in the aminoacylation active site of hmtAlaRS (Supplementary Figure S8A), whose counterpart (Arg128) is responsible for binding ATP, based on the structure of *Archaeoglobus fulgidus* AlaRS (PDB: 3WQY) (Supplementary Figure S8B). Indeed, the resultant hmtAlaRS-R110A exhibited abolished aminoacylation activity (Supplementary Figure S8C). Increasing concentrations of hmtAlaRS-R110A in the aminoacylation reaction of hmtSerRS (hmtSerRS/hmtAlaRS-R110A ranging from 1:1 to 1:8) led to a gradual decrease in hmtSerRS aminoacylation activity, regardless of the substrate being hmtRNA^{Ser}(AGY) (Figure 5D) or hmtRNA^{Ser}(UCN) (Figure 5E). However, aminoacylation activity of hmtSerRS remained nearly unchanged at the presence of various concentrations of purified mature hmtLeuRS (Supplementary Figure S6C), in agreement with the observation of no inter-

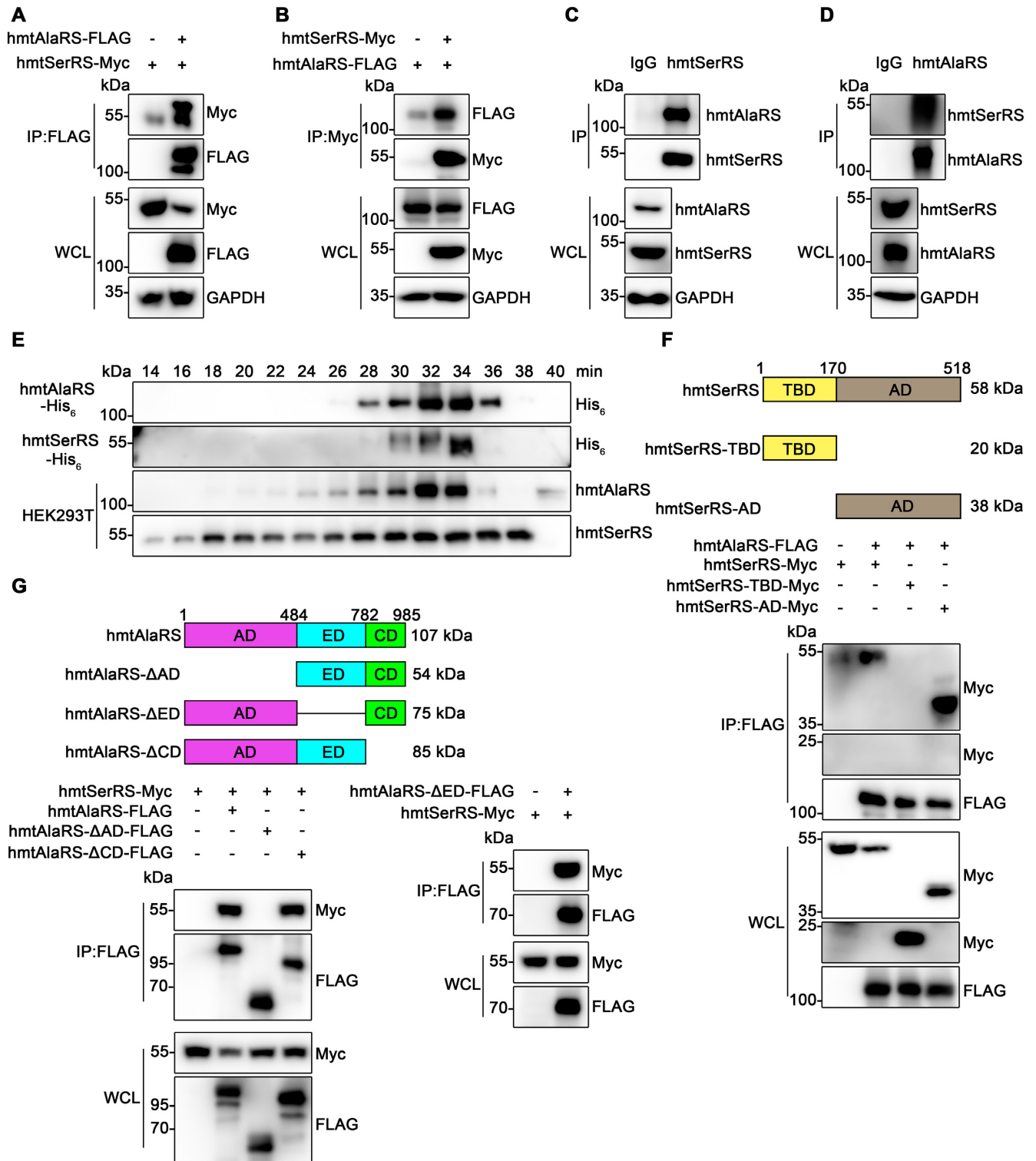


Figure 4. hmtAlaRS interacts with hmtSerRS directly *in vivo*. (A, B) hmtSerRS-Myc and hmtAlaRS-FLAG were coexpressed in HEK293T cells. Co-IP assays using anti-FLAG antibody (A) or anti-Myc antibody (B). (C, D) Co-IP assays of endogenous hmtAlaRS and hmtSerRS immunoprecipitated with anti-hmtSerRS antibody (C) or anti-hmtAlaRS antibody (D) in HEK293T cells. (E) Western blot analysis of elution samples of purified hmtAlaRS-His₆ or hmtSerRS-His₆ or HEK293T WCL by gel filtration on a Superose 6 10/300 GL column. (F) Top panel, the schema of hmtSerRS domain composition. TBD (yellow), tRNA binding domain; AD (gray), aminoacylation domain. Bottom panel, Co-IP analyses using WCL expressing hmtAlaRS-FLAG and various Myc-tagged hmtSerRS mutants as indicated with an anti-FLAG antibody in HEK293T cells. (G) Top panel, the schema of hmtAlaRS domain composition. AD (pink), aminoacylation domain; ED (cyan), editing domain; CD (green), C-terminal domain. Bottom panel, Co-IP analyses using WCL expressing hmtSerRS-Myc and various FLAG-tagged hmtAlaRS mutants as indicated with anti-FLAG antibody in HEK293T cells.

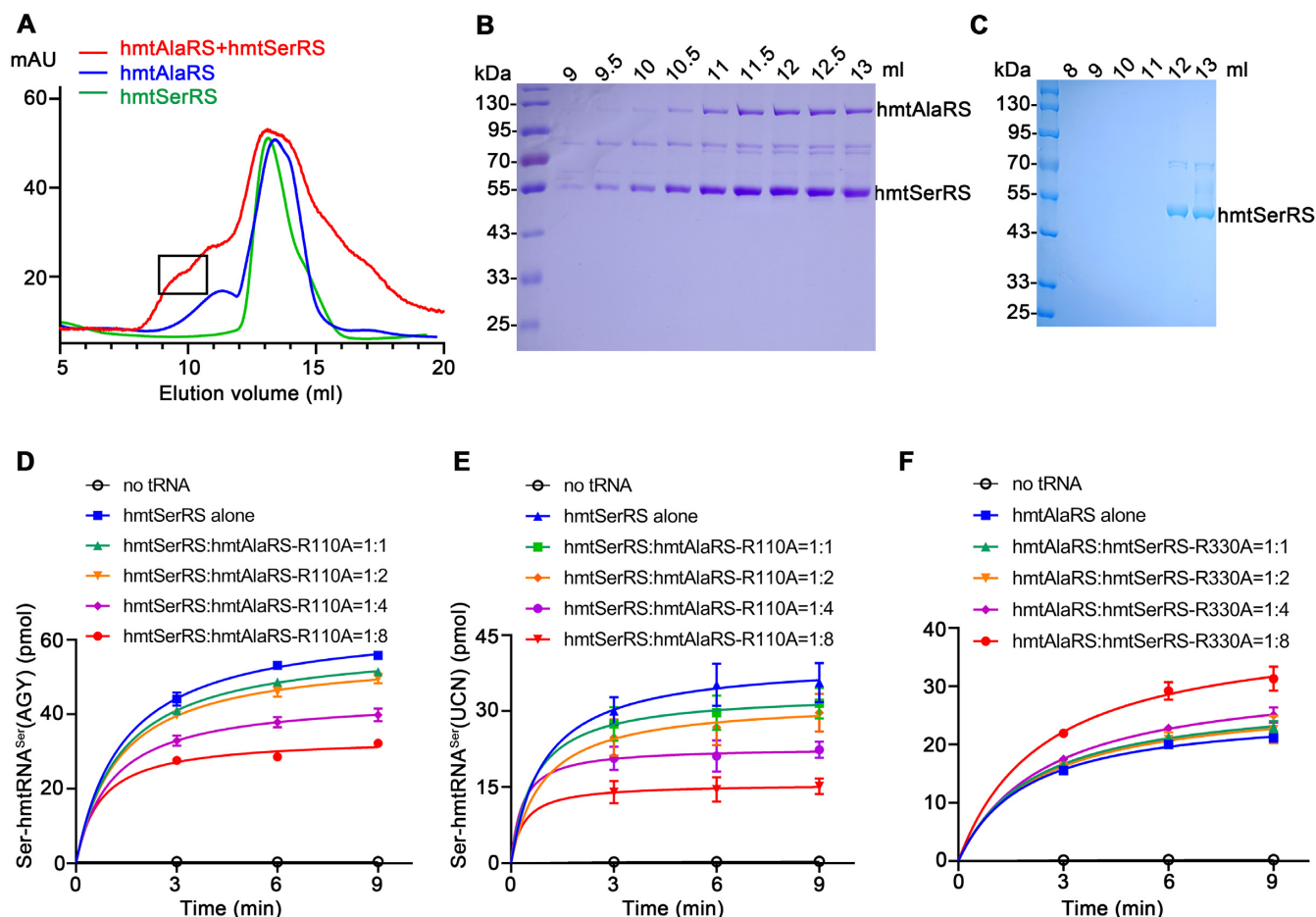


Figure 5. hmtAlaRS–hmtSerRS complex formation affects the respective aminoacylation. (A) Gel filtration analyses of purified hmtAlaRS-His₆, hmtSerRS-His₆ and hmtAlaRS–hmtSerRS complex on Superdex 200. The black box indicates the hmtSerRS–hmtAlaRS complex. (B, C) SDS–PAGE analyses of hmtAlaRS–hmtSerRS complex (B) and hmtSerRS-His₆ alone (C) elution samples. (D, E) Aminoacylation of hmtRNA^{Ser}(AGY) (D) or hmtRNA^{Ser}(UCN) (E) by hmtSerRS in the presence of different concentrations of hmtAlaRS-R110A (hmtSerRS/hmtAlaRS-R110A ranging from 1:1 to 1:8). (F) Aminoacylation of hmtRNA^{Ala} by hmtAlaRS and hmtSerRS-R330A at different concentrations (hmtAlaRS to hmtSerRS-R330A ranging from 1:1 to 1:8). No tRNA was included as a negative control in (D–F). In all the graphs, the data represent the averages of three independent experiments and the corresponding standard deviations.

action between hmtSerRS and hmtLeuRS (Supplementary Figures S6A, B).

Similarly, although whether Ala was misactivated by hmtSerRS has not been experimentally demonstrated, in regard to similar sizes of Ser and Ala, to prevent any potential generation of Ala-AMP by hmtSerRS, we constructed a hmtSerRS-R330A mutant because Arg330 is also an absolutely conserved residue and is responsible for binding ATP (Supplementary Figure S8D), based on the structure of bovine mitochondrial SerRS (PDB: 1WLE) (Supplementary Figure S8E). The tRNA aminoacylation activity of hmtSerRS-R330A was abolished (Supplementary Figure S8F). The purified hmtAlaRS and hmtSerRS-R330A were mixed with different proportions (hmtAlaRS to hmtSerRS-R330A ranging from 1:1 to 1:8), and the aminoacylation of hmtRNA^{Ala} by hmtAlaRS was obviously elevated only in the presence of hmtAlaRS/hmtSerRS-R330A at a 1:8 ratio when compared with that of hmtAlaRS (Figure 5F). hmtAlaRS aminoacylation activity was only slightly increased at lower concentrations of hmtSerRS-R330A (Figure 5F).

Collectively, these results suggested that complex formation between hmtAlaRS and hmtSerRS is able to fine-tune the tRNA charging activity of individual constituents.

Other mito aaRS-containing complexes

As described above, we performed IP-MS analyses of hmtAlaRS, hmtSerRS and hmtThrRS. hmtArgRS was detected in the precipitated samples of hmtThrRS (Supplementary Figure S5D). To understand whether hmtThrRS could interact with hmtArgRS, we performed Co-IP assays in HEK293T cells by overexpressing genes encoding C-terminal FLAG-tagged hmtArgRS (hmtArgRS-FLAG) and C-terminal Myc-tagged hmtThrRS (hmtThrRS-Myc). The results showed that hmtThrRS-Myc could be pulled down by hmtArgRS-FLAG and *vice versa* (Figure 6A, B). hmtArgRS is unique in mito aaRSs because, based on primary sequence alignment, an obvious MTS sequence is undetectable (Supplementary Figure S9A). The very N-terminus of hmtArgRS, Met¹-Leu¹⁷, actually folds into an α -helix, which is a conserved part of the tRNA binding do-

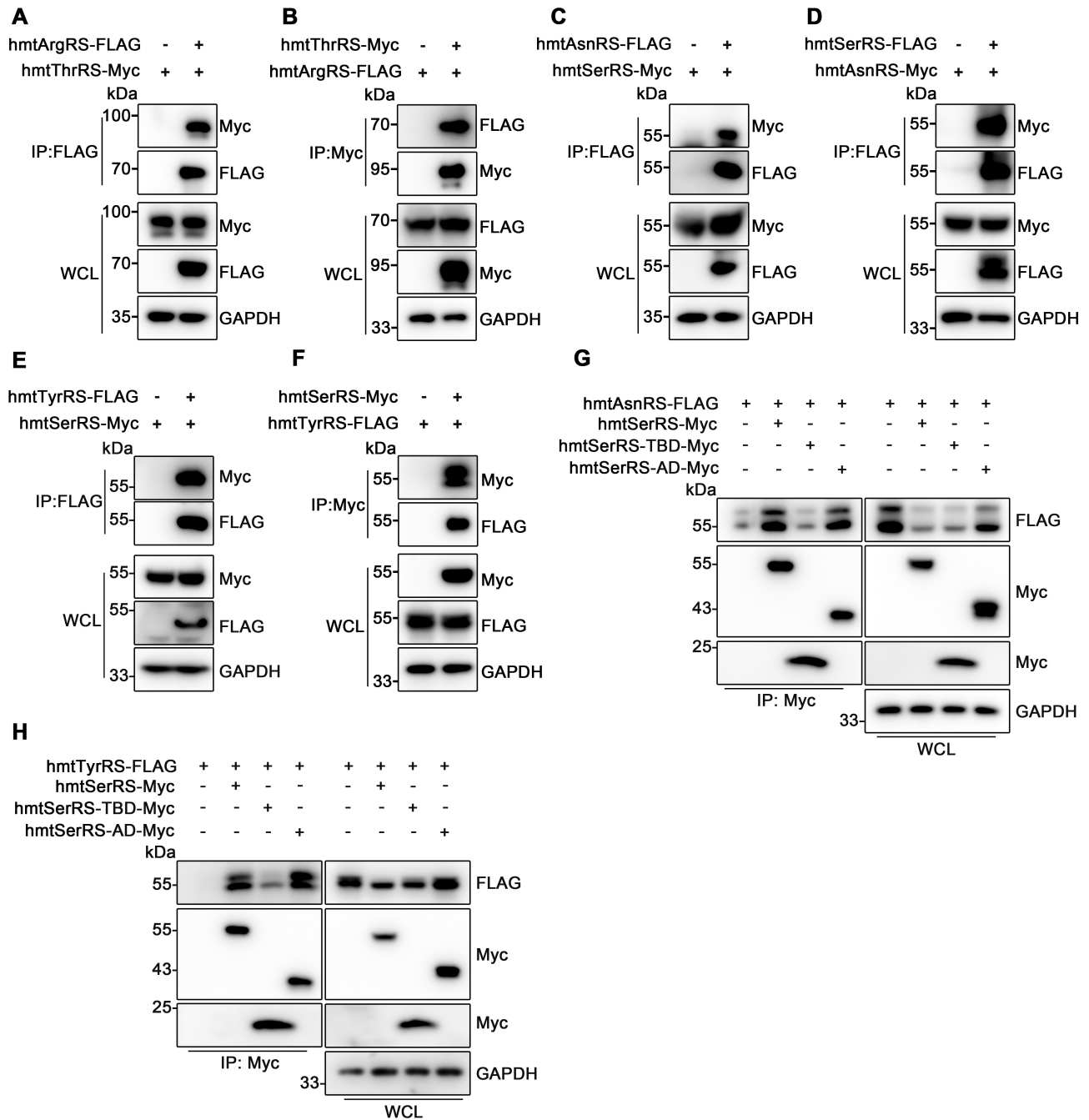


Figure 6. Other mito aaRS-containing complexes. (A, B) HEK293T cells were cotransfected with constructs expressing hmtThrRS-Myc and hmtArgRS-FLAG, and Co-IP was performed with anti-FLAG antibody (A) or anti-Myc antibody (B). (C, D) hmtSerRS interacts with hmtAsnRS. hmtSerRS-Myc was coimmunoprecipitated by hmtAsnRS-FLAG (C), and hmtAsnRS-Myc was also coimmunoprecipitated by hmtSerRS-FLAG (D) using an anti-FLAG antibody in HEK293T cells expressing both proteins. (E, F) HEK293T cells were cotransfected with constructs expressing hmtSerRS-Myc and hmtTyrRS-FLAG, and Co-IP was performed with anti-FLAG antibody (E) or anti-Myc antibody (F). (G) Mapping of the hmtSerRS domain for interaction with hmtAsnRS. Co-IP analyses were performed using WCL expressing hmtAsnRS-FLAG and various Myc-tagged hmtSerRS mutants with an anti-Myc antibody. (H) Mapping of the hmtSerRS domain for interaction with hmtTyrRS. Co-IP analyses were performed using WCL expressing hmtTyrRS-FLAG and various Myc-tagged hmtSerRS mutants with anti-Myc antibody.

main, as reflected by crystal structures of *E. coli* ArgRS (PDB: 4OBY) (72) and *Saccharomyces cerevisiae* ArgRS (PDB: 1F7U) (73) (Supplementary Figure S9B). Consistently, in the structure predicted by AlphaFold 2, this peptide forms an α -helix with high confidence (Supplementary Figure S9B). We have expressed genes encoding full-length hmtArgRS or a series of N-terminal truncated versions of hmtArgRS (including hmtArgRS- Δ N16, the first 16-aa was predicted to be the MTS by Mitoprot (74)); however, they all formed protein aggregates. In *E. coli*, upon coexpression of both His₆-tagged full-length hmtArgRS (hmtArgRS-His₆) and mature hmtThrRS (Leu²⁰-Phe⁷¹⁸) without a tag, we found that hmtThrRS coprecipitated with trace amounts of soluble hmtArgRS-His₆ (Supplementary Figure S9C). The above data clearly suggested that hmtThrRS interacts with hmtArgRS directly *in vivo*. In addition to hmtAlaRS, hmtSerRS and hmtThrRS, we further carried out IP-MS analyses of all other mito aaRSs and thus established a full network of interaction partners of all mito aaRSs (Supplementary Figure S10). We are particularly interested in potential interactions among mito aaRSs. To this end, we indeed found that hmtThrRS was present in the precipitated product of hmtArgRS (Supplementary Figure S10), in line with the above results.

Notably, we found that hmtSerRS was present in the precipitated samples of both hmtAsnRS and hmtTyrRS (Supplementary Figure S10). In addition, hmtAlaRS was also detected in the precipitated samples of hmtTyrRS (Supplementary Figure S10). However, hmtAsnRS and hmtTyrRS were not present in the hmtSerRS-enriched product (Supplementary Figure S5C); hmtTyrRS was not discovered in the hmtAlaRS-enriched samples (Supplementary Figure S5B). Consequently, we examined the interaction of hmtSerRS with hmtAsnRS and hmtTyrRS. We coexpressed hmtSerRS-Myc and C-terminal FLAG-tagged hmtAsnRS (hmtAsnRS-FLAG) in HEK293T cells. Using an anti-FLAG antibody to perform Co-IP, hmtSerRS-Myc was coprecipitated with hmtAsnRS-FLAG (Figure 6C); similarly, hmtAsnRS-Myc was coprecipitated with hmtSerRS-FLAG (Figure 6D). hmtAsnRS has never been expressed and purified in *E. coli*. hmtAsnRS harbors an obvious MTS sequence, which is predicted to be cleaved between Pro²⁴ and Ser²⁵ by Mitoprot (74) (Supplementary Figure S9D). We constructed the predicted mature form of hmtAsnRS (Ser²⁵-Leu⁴⁷⁷); however, it formed inclusion bodies during gene expression in *E. coli*. We coexpressed genes encoding the predicted mature hmtAsnRS with an N-terminal His₆ tag (hmtAsnRS-His₆) and mature hmtSerRS without a tag in *E. coli*. Although hmtAsnRS still formed extensive inclusion bodies and was only marginally soluble in *E. coli* supernatant, hmtSerRS was coprecipitated with hmtAsnRS-His₆ after purification by using Ni-NTA affinity chromatography (Supplementary Figure S9E). These data indicated that hmtSerRS directly interacts with hmtAsnRS *in vivo*.

A similar analysis was performed to investigate the interaction between hmtTyrRS and hmtSerRS. Genes encoding hmtTyrRS with a C-terminal FLAG tag (hmtTyrRS-FLAG) and hmtSerRS-Myc were overexpressed in HEK293T cells, and Co-IP results showed that hmtTyrRS-FLAG interacts with hmtSerRS-Myc using either anti-FLAG antibody (Figure 6E) or anti-Myc anti-

body (Figure 6F). hmtTyrRS has been previously purified and structurally determined (44). By coexpressing genes encoding mature hmtTyrRS (Ala³²-Leu⁴⁷⁷) with a C-terminal His₆ tag (hmtTyrRS-His₆) and mature hmtSerRS without a tag in *E. coli*, we further confirmed the direct interaction between hmtSerRS and hmtTyrRS after Ni-NTA purification (Supplementary Figure S9F). Considering that hmtSerRS directly interacts with multiple mito aaRSs *in vivo*, we further determined the domain for these interactions. Genes encoding hmtSerRS-TBD-Myc or hmtSerRS-AD-Myc were coexpressed with hmtAsnRS-FLAG, and the Co-IP results showed that the aminoacylation domain of hmtSerRS mediates the hmtSerRS-hmtAsnRS interaction (Figure 6G). Similarly, the aminoacylation domain of hmtSerRS was also responsible for the hmtSerRS-hmtTyrRS interaction (Figure 6H). Thus, the catalytic domain of hmtSerRS is the binding site for hmtAlaRS, hmtAsnRS and hmtTyrRS, suggesting that hmtSerRS forms multiple binary complexes with these mito aaRSs but not a core component of a larger complex containing all four mito aaRSs. To exclude the latter hypothesis, we coexpressed genes encoding C-terminal Myc-tagged hmtAlaRS (hmtAlaRS-Myc) and hmtAsnRS-FLAG in HEK293T cells and performed Co-IP with an anti-FLAG antibody. The results showed that hmtAlaRS-Myc could not be pulled down by hmtAsnRS-FLAG (Supplementary Figure S11A). In parallel, hmtAlaRS-Myc could not coprecipitate with hmtTyrRS-FLAG (Supplementary Figure S11B), and hmtAsnRS-Myc could not coprecipitate with hmtTyrRS-FLAG (Supplementary Figure S11C). These results suggested that hmtAlaRS and hmtAsnRS, hmtAlaRS and hmtTyrRS, and hmtAsnRS and hmtTyrRS were not in a quaternary complex using hmtSerRS as a scaffold.

Additionally, hmtCysRS and hmtGluRS were identified in the precipitated samples of each other (Supplementary Figure S10). We tried to explore whether hmtCysRS interacts with hmtGluRS. Therefore, genes encoding hmtCysRS with a C-terminal FLAG tag (hmtCysRS-FLAG) and C-terminal Myc-tagged hmtGluRS (hmtGluRS-Myc) were coexpressed in HEK293T cells. The Co-IP results showed that hmtGluRS-Myc was precipitated by hmtCysRS-FLAG using an anti-FLAG antibody (Supplementary Figure S12A); however, hmtCysRS-FLAG was not coprecipitated by hmtGluRS-Myc using an anti-Myc antibody (Supplementary Figure S12B). Thus, we were uncertain whether the hmtGluRS and hmtCysRS interaction occurs *in vivo*.

In summary, these results suggested that multiple complexes containing at least two mito aaRSs exist. Notably, hmtSerRS interacted with hmtAlaRS, hmtAsnRS and hmtTyrRS using the same aminoacylation domain.

Aminoacylation activity tuning due to the hmtSerRS-hmtTyrRS interaction

Subsequently, we examined whether complex formation of hmtSerRS-hmtTyrRS influences the aminoacylation of individual components. The gene encoding mature hmtTyrRS was expressed in *E. coli* and successfully purified to homogeneity via Ni-NTA purification (Supplementary Figure S13). We initially determined the effect of hmtTyrRS

on hmtSerRS aminoacylation. TyrRS from all sources have hitherto not been reported to misactivate Ser. Indeed, Tyr and Ser exhibit an obvious difference in side chains. Thus, wild-type mature hmtTyrRS was applied in the aminoacylation assay. The purified hmtSerRS was incubated with different concentrations of hmtTyrRS (hmtSerRS/hmtTyrRS ranging from 1:1 to 1:8), and the results showed that the aminoacylation of hmtRNA^{Ser}(AGY) (Figure 7A) or hmtRNA^{Ser}(UCN) (Figure 7B) by hmtSerRS was not affected by hmtTyrRS. However, increasing concentrations of hmtSerRS (hmtTyrRS/hmtSerRS ranging from 1:1 to 1:8) gradually elevated the aminoacylation activity of hmtTyrRS for hmtRNA^{Tyr}, exhibiting the highest activity with an hmtTyrRS/hmtSerRS molar ratio of 1:8 (Figure 7C).

These results showed that the hmtSerRS and hmtTyrRS interaction is able to fine-tune the aminoacylation activity of hmtTyrRS but not hmtSerRS. However, for hmtThrRS-hmtArgRS and hmtSerRS-hmtAsnRS interactions, failure to obtain hmtArgRS and hmtAsnRS made determination of aminoacylation fine-tuning impossible.

DISCUSSION

Mito aaRSs are mainly distributed in the MRG and are likely to facilitate coordinated and efficient mitochondrial mRNA translation

An increasing number of MRG proteins have been identified by IP-MS and further observed by confocal microscopy (45,46,75). Remarkably, several mito aaRSs have been identified in the MRG proteome (45–47), but further confirmation is lacking. Our confocal results showed that all overexpressed mito aaRSs were organized into GRSF1-positive foci. The superresolution fluorescence microscope was further utilized to confirm the colocalization. Obviously, all tested mito aaRSs partly colocalized with GRSF1-containing MRGs. Under superresolution, mito aaRSs are more diffuse than GRSF1 signals, possibly due to the higher abundance of overexpressed aaRSs than at physiological concentrations.

DNA-binding proteins, such as mtSSB (single strand binding protein), TFAM (mitochondrial transcription factor), POLG (DNA polymerase subunit gamma-1), and POLRMT (DNA-directed RNA polymerase), which are involved in mtDNA replication, have been found outside of MRG but present in the nucleoid (10,75). However, MRG constituents are closely related to mitochondrial RNA transcription, processing, maturation and degradation. This phenomenon suggests that the reason for MRG localization is mitochondrial RNA binding capacity. Indeed, mito aaRS mutants deprived of the tRNA binding domain were not apparently colocalized in the MRG, suggesting that tRNA binding domains in mito aaRSs are key determinants in MRG distribution.

Mitochondrial tRNAs are transcribed and processed in the MRG (23). In parallel, mitochondrial mRNAs are mature in the MRG, as evidenced by MRG-localized mRNA metabolism-related proteins, such as GRSF1, members of the FASTK family, and mtPAP (14,18). Furthermore, mitochondrial 12S and 16S rRNAs are also modified in MRG (45). Notably, mitochondrial ribosomal proteins are found

in MRG, suggesting that mitochondrial ribosome assembly and translation initiation occur in these compartments (45). Therefore, it is reasonable that one of the most crucial processes in the tRNA life cycle, tRNA aminoacylation, takes place by MRG-concentrated mito aaRSs. Otherwise, if tRNAs are charged outside of MRG due to peripheral mito aaRSs, it would exhibit disadvantages in mitochondrial mRNA translation. tRNA must be transferred outside of the MRG and then retransported into the MRG, particularly tRNA^{Met}, due to its essential role in mitochondrial translation initiation in the MRG (23). In such cases, the speed of mRNA translation would be compromised. Additionally, the distribution of mito aaRSs in the MRG likely elevates their local concentrations to enhance tRNA charging efficiency. Additionally, as revealed in this study, MRG distribution might enhance local concentration, facilitating the formation of binary aaRS complexes to fine-tune tRNA aminoacylation for several mito aaRSs, leading to a globally coordinated balance of various levels of tRNA charging efficiencies. Therefore, we suggest that localization of mito aaRSs in MRG is perhaps a way to spatially optimize aminoacylation of full sets of mitochondrial tRNAs. Presence of multiple mito aaRS complexes in the MRG may further fine-tune the aminoacylation efficiency by individual aaRS to ensure a harmonized supply of aminoacyl-tRNAs for coordinated and efficient mitochondrial mRNA translation.

Mito aaRSs may form multiple types of aaRS-containing complexes

Using IP-MS analyses, we established an interaction network of all mito aaRSs. Various potential interaction partners were identified, including mitochondrial ribosome proteins. This is reasonable since upon charging, aminoacyl-tRNAs were immediately transported to the ribosome for decoding. Such a tRNA channeling mechanism has been observed in cytoplasmic translation (76). Specifically, several mito aaRSs potentially interact with subunits of ATP synthetase (complex V), which is located in the inner membrane, consistent with the fact that overexpressed mito aaRSs are more diffuse, as observed by superresolution microscopy, and likely reside outside of the MRG to some extent. In fact, such an interaction has been observed between overexpressed hmtTyrRS and complexes I and IV (77); likewise, hmtArgRS and a fraction of hmtLysRS are attached to the inner membrane (48). Additionally, some cytoplasmic proteins were detected in the precipitated samples of various mito aaRSs, perhaps due to the observations that some mito aaRSs carried out some noncanonical functions outside of mitochondria. For example, hmtThrRS has been reported to be involved in Thr-dependent mTORC1 activation in the cytoplasm (49). Moreover, hmtTrpRS has been shown to determine angiogenesis (50). It is also possible that, after cell lysis, a given mito aaRS was able to form a complex with cytoplasmic proteins. For example, using hmtLysRS as a bait, most components of cytoplasmic MSC were enriched, due to the identical p38 binding site between hmtLysRS and cytoplasmic LysRS. Certainly, we cannot exclude the possibility that some proteins are artificially included in the IP-MS assays. Another limitation of

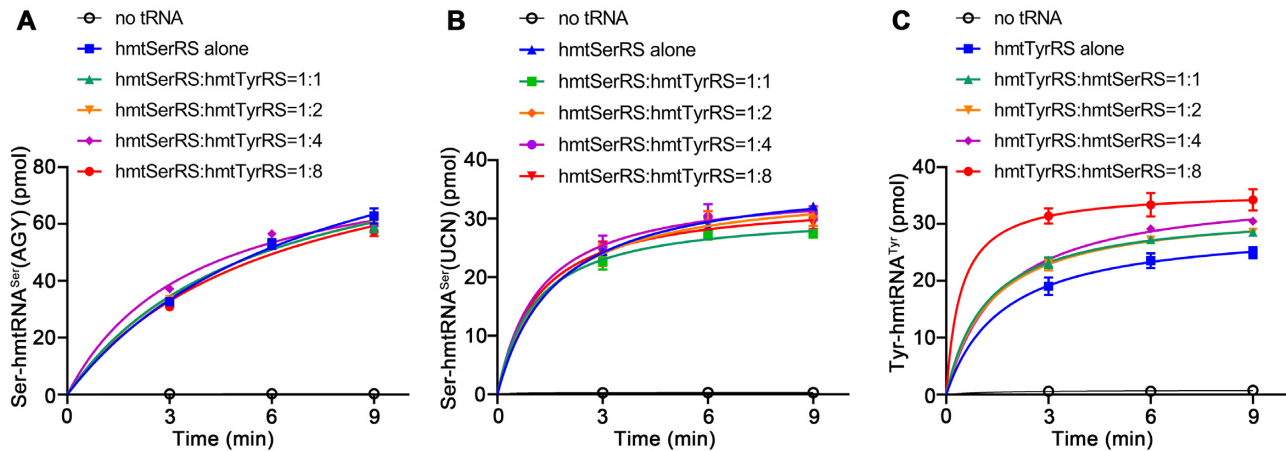


Figure 7. hmtSerRS–hmtTyrRS complex formation fine-tunes the aminoacylation activity of hmtTyrRS. (A, B) Aminoacylation of hmtRNA^{Ser}(AGY) (A) or hmtRNA^{Ser}(UCN) (B) by hmtSerRS in the presence of different amounts of hmtTyrRS (hmtSerRS/hmtTyrRS ranging from 1:1 to 1:8). (C) Aminoacylation of hmtRNA^{Tyr} by hmtTyrRS or in the presence of hmtSerRS in different proportions (hmtTyrRS/hmtSerRS ranging from 1:1 to 1:8). No tRNA was included as a negative control in (A–C). In all the graphs, the data represent the averages of three independent experiments and the corresponding standard deviations.

this method is the potential absence of proteins with small molecular masses due to a lack or inefficiency in proteolysis during MS. In this study, we only focused on the interaction between mito aaRSs. However, the potential interaction between a mito aaRS and a non-aaRS protein was not experimentally investigated in this work and needs to be further confirmed.

Most strikingly, we identified and demonstrated that several mito aaRSs form multiple types of tRNA synthetase complexes. In fact, the existence of a mitochondrial MSC is proposed in 2012 because endogenous hmtTyrRS and hmtGlyRS eluted as a larger complex than their dimers (78), implying that they are components of an undefined complex. Here, we established several interactions between specific mito aaRSs. To the best of our knowledge, this is the first report describing mitochondrial MSC complex components. This is not unexpected considering the widespread presence of MSCs in nature. Due to the bacterial origin of human mitochondria, we compared the bacterial aaRS-harboring complex. In bacteria, three types of aaRS-containing complexes have been identified. In *H. influenzae* and *E. coli*, the *trans*-editing factor YbaK interacts with ProRS to selectively hydrolyze Cys-tRNA^{Pro} due to the lack of specificity of free YbaK to edit correct Cys-tRNA^{Cys} (33,79). This complex is necessary to ensure translational quality control and to simultaneously support translation efficiency. In most bacteria (such as *Thermus thermophilus* and *Helicobacter pylori*), nondiscriminating AspRS and/or GluRS and amidotransferase GatCAB form transamidosomes to catalyze transamidation for the synthesis of Asn-tRNA^{Asn} and/or Gln-tRNA^{Gln} due to a lack of AsnRS and/or GlnRS (80). In addition, in *Deinococcus radiodurans*, one of the two TrpRS types interacts with nitric oxide synthase (NOS) to accelerate the generation of 4-nitro-Trp (33,81). Obviously, each of these bacterial aaRS-containing complexes only contains one aaRS with a non-aaRS partner, and most bacterial aaRSs are present as free forms. Notably, we described here that in human mitochondria,

several aaRS-containing complexes harbor more than one aaRS activity.

For the most extensively studied hmtAlaRS–hmtSerRS complex in this work, the affinity between two synthetases seems to be weak. We are unable to reconstitute a stable complex *in vitro*. Consistently, the majority of endogenous hmtAlaRS still exists in the free form. We cannot exclude the possibility that some yet unidentified factor is able to augment the interaction between hmtAlaRS and hmtSerRS. A similar phenomenon has been observed in human mitochondrial GatCAB, where the interaction between GatA and GatB is dependent on stabilizing function by a small but indispensable nonenzymatic subunit GatC (82). It is also possible that there is a balance between free and complex hmtAlaRS *in vivo*. Under specific stresses, stimuli or physiological or pathological conditions, more hmtAlaRS may be targeted to form or be released from the complex. Such a dynamic between free or complex forms of aaRSs is frequently observed in cytoplasmic MSCs and is usually mediated by phosphorylation at specific sites (29). Despite little description of the noncanonical functions of mito aaRSs, it remains unclear whether mito aaRSs mediate the effect of complex formation on potential nontranslational pathways.

hmtSerRS is the binding partner for multiple mito aaRSs

Unexpectedly, we found that hmtSerRS is able to form a complex with hmtAlaRS, hmtAsnRS and hmtTyrRS. Strikingly, the same catalytic domain of hmtSerRS mediates all the interactions. Indeed, the N-terminal TBD is two long α -helices that have been shown to be critical for binding both hmtRNA^{Ser} substrates (71). If the TBD is used to be involved in protein–protein interactions, tRNA aminoacylation would be compromised due to spatial repulsion. In contrast, the catalytic domain harbors more potential interacting elements. The same catalytic domain of hmtSerRS for various interactions suggested that binding of hmtSerRS

with hmtAlaRS, hmtAsnRS or hmtTyrRS is mutually exclusive and that the possibility of forming a hmtSerRS-centered larger complex containing all four tRNA synthetases is low. In concert with this suggestion, we found no interaction between hmtAlaRS and hmtAsnRS, hmtTyrRS and hmtAsnRS, or hmtAlaRS and hmtTyrRS. In addition, we have recently reported that hmtSerRS forms a direct complex with mitochondrial tRNA 3-methylcytidine modification enzyme METTL8 (51). All these evidences suggest that hmtSerRS pervasively interacts with other proteins, in agreement with the gel filtration data showing that native hmtSerRS is present in entities with various molecular masses.

Our *in vitro* tRNA charging activity determination clearly showed that the aminoacylation activities of hmtAlaRS or hmtSerRS (in the hmtAlaRS–hmtSerRS interaction) and of hmtTyrRS (in the hmtTyrRS–hmtSerRS interaction) are influenced, suggesting that complex formation is able to fine-tune the tRNA charging activity of individual constituents. The obvious alteration was more pronounced with a large amount of another partner, likely stemming from inefficient complex formation *in vitro*, as evidenced in gel filtration analyses. Albeit small alterations in aminoacylation activity due to interaction, the effect on aminoacylation is possibly even larger *in vivo*. On the other hand, small change in activities of mammalian aaRSs sometimes has an obvious effect on translation and cell function. For instance, hmtThrRS-F323C, hmtAspRS-R58G, hmtAspRS-L613F mutants only exhibited mild changes in aminoacylation activities of hmtThrRS or hmtAspRS but caused impaired mitochondrial translation and various mitochondrial diseases (37,83,84). A minor decrease (less than 2-fold) in editing activity of mouse cytoplasmic AlaRS causes the death of Purkinje cells and results in neurodegeneration (85).

hmtSerRS is one of the two tRNA synthetases catalyzing the aminoacylation of two tRNAs. One of the substrates of hmtSerRS, hmtRNA^{Ser} (AGY), is the most peculiar and unstable tRNA in human mitochondria due to the lack of a D-stem and -loop (4). These observations may require a more elaborated tRNA^{Ser} charging regulatory mechanism via interaction of by hmtSerRS with other proteins.

Implication of the mito aaRS complex in the etiology of some mutations of mito aaRSs

More than 300 mutations have been associated with various human disorders (37). In fact, the pathogenesis of most mutations remains unexplored (38). Some mutations at a given aaRS have been shown to influence its own structure or impair aminoacylation, thus constituting the most likely molecular mechanism of disease onset. However, there are mutations without an influence on both the structure and function of the corresponding aaRS (9). The disease-causing mechanism of this kind of mutation is inexplicable. For mito aaRSs that can form complexes, we suggest that mutations at a given aaRS can potentially influence the aminoacylation of another aaRS by influencing the formation of the mito aaRS complex.

In summary, our work revealed that all mito aaRSs were mainly distributed in the MRG. In addition, several mito aaRSs formed multiple complexes with the potential to

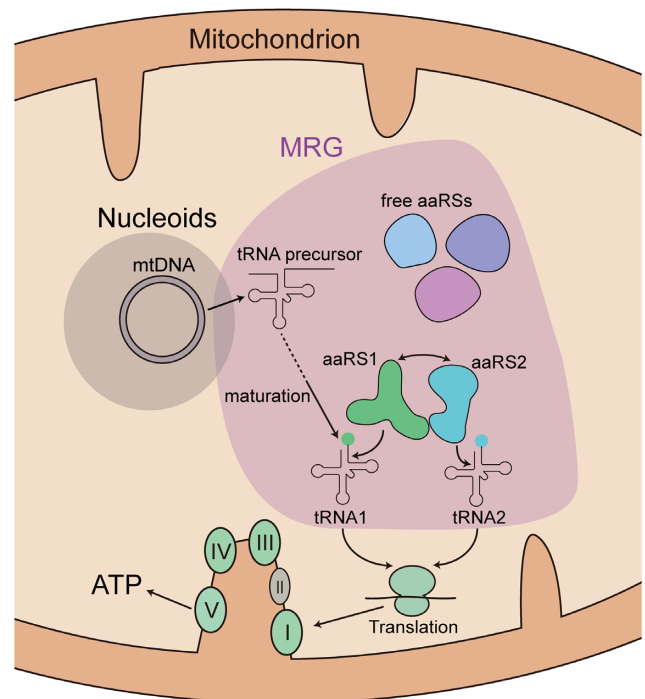


Figure 8. A schematic showing the distribution and complex formation of mito aaRSs. Mito aaRSs were mainly localized in the MRG and formed several complexes, which were able to modulate tRNA aminoacylation activities of specific constituents. The two-way arrow between aaRS1 and aaRS2 (two mito aaRSs in the complex) denoted the functional fine-tuning. Mitochondrial mRNA translation was probably reliant on such a balanced and coordinated supply of aminoacyl-tRNAs to maintain mitochondrial energy homeostasis.

fine-tune tRNA aminoacylation activity of specific tRNA synthetases. This functional regulation might contribute to a coordinated supply of mitochondrial aminoacyl-tRNAs to ensure a balanced and efficient mitochondrial mRNA translation (Figure 8).

DATA AVAILABILITY

All data presented in this study are available within the figures and in the Supplementary data.

SUPPLEMENTARY DATA

Supplementary Data are available at NAR Online.

ACKNOWLEDGEMENTS

We thank Dr. Dan Ye (Fudan University School of Medicine) for providing hmtAspRS expression construct.

FUNDING

National Key Research and Development Program of China [2021YFA1300800, 2021YFC2700903]; Natural Science Foundation of China [91940302, 31870811, 81870896, 32070736, 32271300]; Committee of Science and Technology in Shanghai [22ZR1481300, 22JC1400503]; CAS Project for Young Scientists in Basic Research [YSBR-075].

Funding for open access charge: National Key Research and Development Program of China.

Conflict of interest statement. None declared.

REFERENCES

- Chan, D.C. (2006) Mitochondria: dynamic organelles in disease, aging, and development. *Cell*, **125**, 1241–1252.
- Wallace, D.C. (2005) A mitochondrial paradigm of metabolic and degenerative diseases, aging, and cancer: a dawn for evolutionary medicine. *Annu. Rev. Genet.*, **39**, 359–407.
- Anderson, S., Bankier, A.T., Barrell, B.G., de Bruijn, M.H., Coulson, A.R., Drouin, J., Eperon, I.C., Nierlich, D.P., Roe, B.A., Sanger, F. *et al.* (1981) Sequence and organization of the human mitochondrial genome. *Nature*, **290**, 457–465.
- Suzuki, T., Nagao, A. and Suzuki, T. (2011) Human mitochondrial tRNAs: biogenesis, function, structural aspects, and diseases. *Annu. Rev. Genet.*, **45**, 299–329.
- Vercellino, I. and Sazanov, L.A. (2022) The assembly, regulation and function of the mitochondrial respiratory chain. *Nat. Rev. Mol. Cell Biol.*, **23**, 141–161.
- Peng, G.X., Zhang, Y., Wang, Q.Q., Li, Q.R., Xu, H., Wang, E.D. and Zhou, X.L. (2021) The human tRNA taurine modification enzyme GTPBP3 is an active GTPase linked to mitochondrial diseases. *Nucleic Acids Res.*, **49**, 2816–2834.
- Zhou, J.B., Wang, Y., Zeng, Q.Y., Meng, S.X., Wang, E.D. and Zhou, X.L. (2020) Molecular basis for t⁶A modification in human mitochondria. *Nucleic Acids Res.*, **48**, 3181–3194.
- Antonellis, A. and Green, E.D. (2008) The role of aminoacyl-tRNA synthetases in genetic diseases. *Annu. Rev. Genomics Hum. Genet.*, **9**, 87–107.
- Zeng, Q.Y., Peng, G.X., Li, G., Zhou, J.B., Zheng, W.Q., Xue, M.Q., Wang, E.D. and Zhou, X.L. (2019) The G3-U70-independent tRNA recognition by human mitochondrial alanyl-tRNA synthetase. *Nucleic Acids Res.*, **47**, 3072–3085.
- Bogenhagen, D.F., Rousseau, D. and Burke, S. (2008) The layered structure of human mitochondrial DNA nucleoids. *J. Biol. Chem.*, **283**, 3665–3675.
- Kukat, C., Davies, K.M., Wurm, C.A., Spähr, H., Bonekamp, N.A., Kühl, I., Joos, F., Polosa, P.L., Park, C.B., Posse, V. *et al.* (2015) Cross-strand binding of TFAM to a single mtDNA molecule forms the mitochondrial nucleoid. *Proc. Natl Acad. Sci. U.S.A.*, **112**, 11288–11293.
- Holzmann, J., Frank, P., Löffler, E., Bennett, K.L., Gerner, C. and Rossmann, W. (2008) RNase P without RNA: identification and functional reconstitution of the human mitochondrial tRNA processing enzyme. *Cell*, **135**, 462–474.
- Brzezniak, L.K., Bijata, M., Szczesny, R.J. and Stepien, P.P. (2011) Involvement of human ELAC2 gene product in 3' end processing of mitochondrial tRNAs. *RNA Biol.*, **8**, 616–626.
- Jourdain, A.A., Koppen, M., Wydro, M., Rodley, C.D., Lightowlers, R.N., Chrzanoska-Lightowlers, Z.M. and Martinou, J.C. (2013) GRSF1 regulates RNA processing in mitochondrial RNA granules. *Cell Metab.*, **17**, 399–410.
- Antonicka, H., Sasarman, F., Nishimura, T., Paupe, V. and Shoubridge, E.A. (2013) The mitochondrial RNA-binding protein GRSF1 localizes to RNA granules and is required for posttranscriptional mitochondrial gene expression. *Cell Metab.*, **17**, 386–398.
- Tu, Y.T. and Barrientos, A. (2015) The human mitochondrial DEAD-Box protein DDX28 resides in RNA granules and functions in mitoribosome assembly. *Cell Rep.*, **10**, 854–864.
- Iborra, F.J., Kimura, H. and Cook, P.R. (2004) The functional organization of mitochondrial genomes in human cells. *BMC Biol.*, **2**, 9.
- Jourdain, A.A., Koppen, M., Rodley, C.D., Maundrell, K., Gueguen, N., Reynier, P., Guaras, A.M., Enriquez, J.A., Anderson, P., Simarro, M. *et al.* (2015) A mitochondria-specific isoform of FASTK is present in mitochondrial RNA granules and regulates gene expression and function. *Cell Rep.*, **10**, 1110–1121.
- Wilson, W.C., Hornig-Do, H.T., Bruni, F., Chang, J.H., Jourdain, A.A., Martinou, J.C., Falkenberg, M., Spähr, H., Larsson, N.G., Lewis, R.J. *et al.* (2014) A human mitochondrial poly(A) polymerase mutation reveals the complexities of post-transcriptional mitochondrial gene expression. *Hum. Mol. Genet.*, **23**, 6345–6355.
- Lee, K.W., Okot-Kotber, C., LaComb, J.F. and Bogenhagen, D.F. (2013) Mitochondrial ribosomal RNA (rRNA) methyltransferase family members are positioned to modify nascent rRNA in foci near the mitochondrial DNA nucleoid. *J. Biol. Chem.*, **288**, 31386–31399.
- Jourdain, A.A., Boehm, E., Maundrell, K. and Martinou, J.C. (2016) Mitochondrial RNA granules: compartmentalizing mitochondrial gene expression. *J. Cell Biol.*, **212**, 611–614.
- Borowski, L.S., Dziembowski, A., Hejnowicz, M.S., Stepien, P.P. and Szczesny, R.J. (2013) Human mitochondrial RNA decay mediated by PNPase-hSuv3 complex takes place in distinct foci. *Nucleic Acids Res.*, **41**, 1223–1240.
- Pearce, S.F., Rebelo-Guiomar, P., D'Souza, A.R., Powell, C.A., Van Haute, L. and Minczuk, M. (2017) Regulation of mammalian mitochondrial gene expression: recent advances. *Trends Biochem. Sci.*, **42**, 625–639.
- Eriani, G., Delarue, M., Gangloff, J. and Moras, D. (1990) Partition of tRNA synthetases into two classes based on mutually exclusive sets of sequence motifs. *Nature*, **347**, 203–206.
- Bonnefond, L., Fender, A., Rudinger-Thirion, J., Giege, R., Florentz, C. and Sissler, M. (2005) Toward the full set of human mitochondrial aminoacyl-tRNA synthetases: characterization of AspRS and TyrRS. *Biochemistry*, **44**, 4805–4816.
- Guo, M., Schimmel, P. and Yang, X.L. (2010) Functional expansion of human tRNA synthetases achieved by structural inventions. *FEBS Lett.*, **584**, 434–442.
- Cho, H.Y., Maeng, S.J., Cho, H.J., Choi, Y.S., Chung, J.M., Lee, S., Kim, H.K., Kim, J.H., Eom, C.Y., Kim, Y.G. *et al.* (2015) Assembly of multi-tRNA synthetase complex via heterotetrameric glutathione transferase-homology domains. *J. Biol. Chem.*, **290**, 29313–29328.
- Kerjan, P., Cerini, C., Sémériva, M. and Mirande, M. (1994) The multi-enzyme complex containing nine aminoacyl-tRNA synthetases is ubiquitous from *Drosophila* to mammals. *Biochim. Biophys. Acta*, **1199**, 293–297.
- Hyeon, D.Y., Kim, J.H., Ahn, T.J., Cho, Y., Hwang, D. and Kim, S. (2019) Evolution of the multi-tRNA synthetase complex and its role in cancer. *J. Biol. Chem.*, **294**, 5340–5351.
- Rho, S.B., Kim, M.J., Lee, J.S., Seol, W., Motegi, H., Kim, S. and Shiba, K. (1999) Genetic dissection of protein-protein interactions in multi-tRNA synthetase complex. *Proc. Natl Acad. Sci. U.S.A.*, **96**, 4488–4493.
- Fu, Y., Kim, Y., Jin, K.S., Kim, H.S., Kim, J.H., Wang, D., Park, M., Jo, C.H., Kwon, N.H., Kim, D. *et al.* (2014) Structure of the ArgRS-GlnRS-AIMP1 complex and its implications for mammalian translation. *Proc. Natl Acad. Sci. U.S.A.*, **111**, 15084–15089.
- Cho, H.Y., Lee, H.J., Choi, Y.S., Kim, D.K., Jin, K.S., Kim, S. and Kang, B.S. (2019) Symmetric assembly of a decameric subcomplex in human multi-tRNA synthetase complex via interactions between glutathione transferase-homology domains and aspartyl-tRNA synthetase. *J. Mol. Biol.*, **431**, 4475–4496.
- Hausmann, C.D. and Ibba, M. (2008) Aminoacyl-tRNA synthetase complexes: molecular multitasking revealed. *FEMS Microbiol. Rev.*, **32**, 705–721.
- Hausmann, C.D. and Ibba, M. (2008) Structural and functional mapping of the archaeal multi-aminoacyl-tRNA synthetase complex. *FEBS Lett.*, **582**, 2178–2182.
- Galani, K., Grosshans, H., Deinert, K., Hurt, E.C. and Simos, G. (2001) The intracellular location of two aminoacyl-tRNA synthetases depends on complex formation with Arc1p. *EMBO J.*, **20**, 6889–6898.
- Guo, M. and Schimmel, P. (2013) Essential nontranslational functions of tRNA synthetases. *Nat. Chem. Biol.*, **9**, 145–153.
- Moulinier, L., Ripp, R., Castillo, G., Poch, O. and Sissler, M. (2017) MiSynPat: An integrated knowledge base linking clinical, genetic, and structural data for disease-causing mutations in human mitochondrial aminoacyl-tRNA synthetases. *Hum. Mutat.*, **38**, 1316–1324.
- Sissler, M., Gonzalez-Serrano, L.E. and Westhof, E. (2017) Recent advances in mitochondrial aminoacyl-tRNA synthetases and disease. *Trends Mol. Med.*, **23**, 693–708.
- Neupert, W. and Herrmann, J.M. (2007) Translocation of proteins into mitochondria. *Annu. Rev. Biochem.*, **76**, 723–749.
- Carapito, C., Kuhn, L., Karim, L., Rompais, M., Rabilloud, T., Schwenzer, H. and Sissler, M. (2017) Two proteomic methodologies

- for defining N-termini of mature human mitochondrial aminoacyl-tRNA synthetases. *Methods*, **113**, 111–119.
41. Garin, S., Levi, O., Cohen, B., Golani-Armon, A. and Arava, Y.S. (2020) Localization and RNA binding of mitochondrial aminoacyl tRNA synthetases. *Genes*, **11**, 1185.
 42. Klipcan, L., Moor, N., Finarov, I., Kessler, N., Sukhanova, M. and Safro, M.G. (2012) Crystal structure of human mitochondrial PheRS complexed with tRNA^{Phe} in the active “open” state. *J. Mol. Biol.*, **415**, 527–537.
 43. Neuenfeldt, A., Lorber, B., Ennifar, E., Gaudry, A., Sauter, C., Sissler, M. and Florentz, C. (2013) Thermodynamic properties distinguish human mitochondrial aspartyl-tRNA synthetase from bacterial homolog with same 3D architecture. *Nucleic Acids Res.*, **41**, 2698–2708.
 44. Bonnefond, L., Frugier, M., Touzé, E., Lorber, B., Florentz, C., Giegé, R., Sauter, C. and Rudinger-Thirion, J. (2007) Crystal structure of human mitochondrial tyrosyl-tRNA synthetase reveals common and idiosyncratic features. *Structure*, **15**, 1505–1516.
 45. Antonicka, H. and Shoubridge, E.A. (2015) Mitochondrial RNA granules are centers for posttranscriptional RNA processing and ribosome biogenesis. *Cell Rep.*, **10**, 920–932.
 46. Antonicka, H., Choquet, K., Lin, Z.Y., Gingras, A.C., Kleinman, C.L. and Shoubridge, E.A. (2017) A pseudouridine synthase module is essential for mitochondrial protein synthesis and cell viability. *EMBO Rep.*, **18**, 28–38.
 47. Zaganelli, S., Rebelo-Guimar, P., Maundrell, K., Rozanska, A., Pierredon, S., Powell, C.A., Jourdain, A.A., Hulo, N., Lightowers, R.N., Chrzanowska-Lightowers, Z.M. *et al.* (2017) The pseudouridine synthase RPUSD4 is an essential component of mitochondrial RNA granules. *J. Biol. Chem.*, **292**, 4519–4532.
 48. Gonzalez-Serrano, L.E., Karim, L., Pierre, F., Schwenzler, H., Rotig, A., Munnich, A. and Sissler, M. (2018) Three human aminoacyl-tRNA synthetases have distinct sub-mitochondrial localizations that are unaffected by disease-associated mutations. *J. Biol. Chem.*, **293**, 13604–13615.
 49. Kim, S.H., Choi, J.H., Wang, P., Go, C.D., Hesketh, G.G., Gingras, A.C., Jafarnejad, S.M. and Sonenberg, N. (2021) Mitochondrial threonyl-tRNA synthetase TARS2 is required for threonine-sensitive mTORC1 activation. *Mol. Cell*, **81**, 398–407.
 50. Wang, M., Sips, P., Khin, E., Rotival, M., Sun, X., Ahmed, R., Widjaja, A.A., Schafer, S., Yusoff, P., Choksi, P.K. *et al.* (2016) Wars2 is a determinant of angiogenesis. *Nat. Commun.*, **7**, 12061.
 51. Huang, M.H., Peng, G.X., Mao, X.L., Wang, J.T., Zhou, J.B., Zhang, J.H., Chen, M., Wang, E.D. and Zhou, X.L. (2022) Molecular basis for human mitochondrial tRNA m³C modification by alternatively spliced METTL8. *Nucleic Acids Res.*, **50**, 4012–4028.
 52. Wang, Y., Zhou, X.L., Ruan, Z.R., Liu, R.J., Eriani, G. and Wang, E.D. (2016) A human disease-causing point mutation in mitochondrial threonyl-tRNA synthetase induces both structural and functional defects. *J. Biol. Chem.*, **291**, 6507–6520.
 53. Wang, Y., Zhou, J.B., Zeng, Q.Y., Wu, S., Xue, M.Q., Fang, P., Wang, E.D. and Zhou, X.L. (2020) Hearing impairment-associated KARS mutations lead to defects in aminoacylation of both cytoplasmic and mitochondrial tRNA^{Lys}. *Sci. China Life Sci.*, **63**, 1227–1239.
 54. Yao, Y.N., Wang, L., Wu, X.F. and Wang, E.D. (2003) Human mitochondrial leucyl-tRNA synthetase with high activity produced from *Escherichia coli*. *Protein Expr. Purif.*, **30**, 112–116.
 55. Wu, H., Wei, T., Yu, B., Cheng, R., Huang, F., Lu, X., Yan, Y., Wang, X., Liu, C. and Zhu, B. (2021) A single mutation attenuates both the transcription termination and RNA-dependent RNA polymerase activity of T7 RNA polymerase. *RNA Biol.*, **18**, 451–466.
 56. Wang, J.T., Zhou, J.B., Mao, X.L., Zhou, L., Chen, M., Zhang, W., Wang, E.D. and Zhou, X.L. (2022) Commonality and diversity in tRNA substrate recognition in t⁶A biogenesis by eukaryotic KEOs. *Nucleic Acids Res.*, **50**, 2223–2239.
 57. Jorgensen, R., Søgaard, T.M., Rossing, A.B., Martensen, P.M. and Justesen, J. (2000) Identification and characterization of human mitochondrial tryptophanyl-tRNA synthetase. *J. Biol. Chem.*, **275**, 16820–16826.
 58. Dias, J., Octobre, G., Kobbi, L., Comisso, M., Flisiak, S. and Mirande, M. (2012) Activation of human mitochondrial lysyl-tRNA synthetase upon maturation of its premitochondrial precursor. *Biochemistry*, **51**, 909–916.
 59. Xie, W., Nangle, L.A., Zhang, W., Schimmel, P. and Yang, X.L. (2007) Long-range structural effects of a Charcot-Marie-Tooth disease-causing mutation in human glycyl-tRNA synthetase. *Proc. Natl Acad. Sci. U.S.A.*, **104**, 9976–9981.
 60. Ofir-Birin, Y., Fang, P., Bennett, S.P., Zhang, H.M., Wang, J., Rachmin, I., Shapiro, R., Song, J., Dagan, A., Pozo, J. *et al.* (2013) Structural switch of lysyl-tRNA synthetase between translation and transcription. *Mol. Cell*, **49**, 30–42.
 61. Jumper, J., Evans, R., Pritzel, A., Green, T., Figurnov, M., Ronneberger, O., Tunyasuvunakool, K., Bates, R., Zidek, A., Potapenko, A. *et al.* (2021) Highly accurate protein structure prediction with AlphaFold. *Nature*, **596**, 583–589.
 62. Varadi, M., Anyango, S., Deshpande, M., Nair, S., Natassia, C., Yordanova, G., Yuan, D., Stroe, O., Wood, G., Laydon, A. *et al.* (2022) AlphaFold Protein Structure Database: massively expanding the structural coverage of protein-sequence space with high-accuracy models. *Nucleic Acids Res.*, **50**, D439–D444.
 63. Mudge, S.J., Williams, J.H., Eyre, H.J., Sutherland, G.R., Cowan, P.J. and Power, D.A. (1998) Complex organisation of the 5′-end of the human glycine tRNA synthetase gene. *Gene*, **209**, 45–50.
 64. Tolkunova, E., Park, H., Xia, J., King, M.P. and Davidson, E. (2000) The human lysyl-tRNA synthetase gene encodes both the cytoplasmic and mitochondrial enzymes by means of an unusual alternative splicing of the primary transcript. *J. Biol. Chem.*, **275**, 35063–35069.
 65. Francin, M., Kaminska, M., Kerjan, P. and Mirande, M. (2002) The N-terminal domain of mammalian lysyl-tRNA synthetase is a functional tRNA-binding domain. *J. Biol. Chem.*, **277**, 1762–1769.
 66. Roy, H., Ling, J., Alfonso, J. and Ibba, M. (2005) Loss of editing activity during the evolution of mitochondrial phenylalanyl-tRNA synthetase. *J. Biol. Chem.*, **280**, 38186–38192.
 67. Ye, Q., Wang, M., Fang, Z.P., Ruan, Z.R., Ji, Q.Q., Zhou, X.L. and Wang, E.D. (2015) Degenerate connective polypeptide 1 (CPI) domain from human mitochondrial leucyl-tRNA synthetase. *J. Biol. Chem.*, **290**, 24391–24402.
 68. Lue, S.W. and Kelley, S.O. (2005) An aminoacyl-tRNA synthetase with a defunct editing site. *Biochemistry*, **44**, 3010–3016.
 69. Sommerville, E.W., Zhou, X.L., Oláhová, M., Jenkins, J., Euro, L., Konovalova, S., Hilander, T., Pyle, A., He, L., Habeebu, S. *et al.* (2019) Instability of the mitochondrial alanyl-tRNA synthetase underlies fatal infantile-onset cardiomyopathy. *Hum. Mol. Genet.*, **28**, 258–268.
 70. Hilander, T., Zhou, X.L., Konovalova, S., Zhang, F.P., Euro, L., Chilov, D., Poutanen, M., Chihade, J., Wang, E.D. and Tynynmaa, H. (2018) Editing activity for eliminating mischarged tRNAs is essential in mammalian mitochondria. *Nucleic Acids Res.*, **46**, 849–860.
 71. Chinnaronk, S., Gravers Jeppesen, M., Suzuki, T., Nyborg, J. and Kovalov, K. (2005) Dual-mode recognition of noncanonical tRNAs^{Ser} by seryl-tRNA synthetase in mammalian mitochondria. *EMBO J.*, **24**, 3369–3379.
 72. Bi, K., Zheng, Y., Gao, F., Dong, J., Wang, J., Wang, Y. and Gong, W. (2014) Crystal structure of *E. coli* arginyl-tRNA synthetase and ligand binding studies revealed key residues in arginine recognition. *Protein Cell*, **5**, 151–159.
 73. Delagoutte, B., Moras, D. and Cavarelli, J. (2000) tRNA aminoacylation by arginyl-tRNA synthetase: induced conformations during substrates binding. *EMBO J.*, **19**, 5599–5610.
 74. Claros, M.G. and Vincens, P. (1996) Computational method to predict mitochondrially imported proteins and their targeting sequences. *Eur. J. Biochem.*, **241**, 779–786.
 75. Hensen, F., Potter, A., van Esveld, S.L., Tarrés-Solé, A., Chakraborty, A., Solà, M. and Spelbrink, J.N. (2019) Mitochondrial RNA granules are critically dependent on mtDNA replication factors Twinkle and mtSSB. *Nucleic Acids Res.*, **47**, 3680–3698.
 76. Sivaram, P. and Deutscher, M.P. (1990) Existence of two forms of rat liver arginyl-tRNA synthetase suggests channeling of aminoacyl-tRNA for protein synthesis. *Proc. Natl Acad. Sci. U.S.A.*, **87**, 3665–3669.
 77. Jin, X., Zhang, Z., Nie, Z., Wang, C., Meng, F., Yi, Q., Chen, M., Sun, J., Zou, J., Jiang, P. *et al.* (2021) An animal model for mitochondrial tyrosyl-tRNA synthetase deficiency reveals links between oxidative phosphorylation and retinal function. *J. Biol. Chem.*, **296**, 100437.
 78. Sasarman, F., Nishimura, T., Thiffault, I. and Shoubridge, E.A. (2012) A novel mutation in YARS2 causes myopathy with lactic acidosis and sideroblastic anemia. *Hum. Mutat.*, **33**, 1201–1206.

79. An,S. and Musier-Forsyth,K. (2005) Cys-tRNA^{Pro} editing by *Haemophilus influenzae* YbaK via a novel synthetase.YbaK.tRNA ternary complex. *J. Biol. Chem.*, **280**, 34465–34472.
80. Bailly,M., Blaise,M., Lorber,B., Becker,H.D. and Kern,D. (2007) The transamidosome: a dynamic ribonucleoprotein particle dedicated to prokaryotic tRNA-dependent asparagine biosynthesis. *Mol. Cell*, **28**, 228–239.
81. Buddha,M.R., Keery,K.M. and Crane,B.R. (2004) An unusual tryptophanyl tRNA synthetase interacts with nitric oxide synthase in *Deinococcus radiodurans*. *Proc. Natl Acad. Sci. U.S.A.*, **101**, 15881–15886.
82. Nagao,A., Suzuki,T., Katoh,T., Sakaguchi,Y. and Suzuki,T. (2009) Biogenesis of glutamyl-mt tRNA^{Gln} in human mitochondria. *Proc. Natl Acad. Sci. U.S.A.*, **106**, 16209–16214.
83. Zheng,W.Q., Pedersen,S.V., Thompson,K., Bellacchio,E., French,C.E., Munro,B., Pearson,T.S., Vogt,J., Diodato,D., Diemer,T. *et al.* (2022) Elucidating the molecular mechanisms associated with *TARS2*-related mitochondrial disease. *Hum. Mol. Genet.*, **31**, 523–534.
84. van Berge,L., Kevenaer,J., Polder,E., Gaudry,A., Florentz,C., Sissler,M., van der Knaap,M.S. and Scheper,G.C. (2013) Pathogenic mutations causing LBSL affect mitochondrial aspartyl-tRNA synthetase in diverse ways. *Biochem J.*, **450**, 345–350.
85. Lee,J.W., Beebe,K., Nangle,L.A., Jang,J., Longo-Guess,C.M., Cook,S.A., Davisson,M.T., Sundberg,J.P., Schimmel,P. and Ackerman,S.L. (2006) Editing-defective tRNA synthetase causes protein misfolding and neurodegeneration. *Nature*, **443**, 50–55.